Responses to the Referee

General comments:

The topic of the paper is relevant, but the study has limitations and weaknesses that should be tackled.

5 **Specific comments:**

Comment 1: The literature review in the Introduction is wide, but not well organized and structured. I suggest reorganizing and rephrasing it to improve readability.

Response: Thanks for the referee's suggestion for the Introduction. We have reorganized this section in our revised version.

10 **Comment 2: In the Introduction it is mentioned that "It has been proven in statistical science that different results are obtained using different choices of ILR balances", but no references are provided to support this claim. Please, add references of works where the influence of the choice of ILR balances on the results is demonstrated.**

Response: Thanks for the referee's suggestion. We have added the references and introduced more details about the choice of ILR balances.

15

P3L85: *"It has been proven in statistical science that different results are obtained using different ILR balances. For example, Fiserova and Hron (2011) reported that different balances generated different covariance structures. Moreover, the choice of SBP is related to hypotheses, research questions of interest, or the context of the data analysis (Coenders et al., 2017; Facevicova et al., 2018). Thus, the option of a specific SBP for compositions is crucial for the intended interpretation of*

20 *coordinates (Fiserova and Hron, 2011)."*

Comment 3: In equations (7) and (8), are M_i and P_i (D-1)- vectors? If so, the expressions (7) and (8) should account for that. Otherwise, their meaning should be better explained.

Response: Thanks for the referee's suggestion for the equations. M_i and P_i are not D-1 vectors, instead, they are measured

25 and predicted values for raw data (i.e., sand, silt and clay), respectively. This is because we used these indicators (ME, RMSE) to measure prediction bias and accuracy compared with the raw data (D), P_i is the predicted value that back-transformed to the real space. Therefore, M_i and P_i are D vectors (D = 3) for sand, silt and clay. We have improved this part in our revised version.

30 **P8L218:** *"where M_i and P_i are the measured and predicted values of the ith sample for sand, silt and clay."*

Comment 4: Are the differences found in the indicators significant? The comparisons reported (for example in Sections 3.2, 4.1 and 4.2) should be based on statistical tests to verify the statistical significance of the differences observed in the indicators. The significance of the differences should also be taken into consideration in the grading of the three

SBP at the end of Section 3.2, otherwise the results shown in Figure 5 may be misleading.

Response: Thank you for your suggestion regarding the statistical significance test for the results of different models. Based on a 30-times independent dataset validation method, we performed a Diebold–Mariano test (Diebold and Mariano, 1995; Harvey et al., 1997) for the two models. The p-values of MEs and RMSEs of sand, silt, and clay fractions, and also Ads, were shown in the following tables. The null hypothesis is that the two methods have the same level of prediction accuracy, and the alternative hypothesis is that method 1 and method 2 have different levels of accuracy (when $p<0.05$, the null hypothesis is rejected). The significance tests showed that most p-values were significant, expect for the ME of sand fractions. The differences were reflected in not only different models (GLM and RF), but also in different SBPs when using the same model. For the RF model, combining RK or not is not significant, which may be because RF has less uncertainty, or because the RF algorithm is robust to ILR data and residuals. For Fig. 5, we used the mean value of the 30-times results. We have adopted your suggestion and recalculated these indicators based on the significance test. The basic principle is that if the results of different SBPs were not significant, then the same score was used; if they were significant, different scores were used based on model performance. The new result was shown in Fig. 5, and we found that different SBPs delivered different performances in GLM and RF. In bias assessment, SBP1 performed best. Regarding accuracy, SBP3 and SBP1 delivered a good performance for GLM and RF, respectively. Moreover, in the comprehensive assessment, SBP1 still performed best out of the three SBPs according to SUM6, which is the same as we did before. In summary, this evaluation method is designed to evaluate the performance of different SBPs based on the predicted results and significance test. Using the ranking score in Fig. 5, we demonstrated that different SBP balances generated significant differences, and compositional balance should be considered when mapping soil PSFs. We also included this in the Conclusion Section. Therefore, we have improved this part in our revised version and Supplementary Material.

P8L204: *"Moreover, the Diebold–Mariano test (Diebold and Mariano, 1995; Harvey et al., 1997) was used to verify the statistical significance of the differences among the models."*

P11L276: *"To assess the accuracy of the different models, the Diebold–Mariano test was used, which showed that the statistical differences of most models were significant. This significance was reflected not only in different models (GLM and RF), but also in different SBPs when using the same model (Tables S6.1–S6.7)."*

P12L294: *"The model performances were different for the three SBPs. To better evaluate model performance using the different SBP balances, we graded each box from 1 to 3 based on the predicted results and Diebold¬–Mariano test results— the final results are shown in Fig. 5. SBP1 performed best in terms of bias, with the lowest ME score of all models, except for GLMRK (Fig. 5a). With respect to the model accuracy assessment, there was no apparent pattern, but the accuracy could be considered hierarchically: (1) for the GLM, SBP3 performed better than the other two SBP methods, and SBP1 performed well when combined with RK (GLMRK); (2) for RF, SBP1 produced the best result. However, the introduction of RK resulted*

in the SBP2 and SBP3 performing well (Fig. 5b). In addition, SBP3 and SBP1 delivered a better performance for GLM and RF, respectively (Figs. 5c–5e). Finally, in a comprehensive assessment, SBP1 performed best out of the three SBPs according to SUM6 (Fig. 5f). More details and calculations can be found in the Supplementary Material (Table S4.1)."
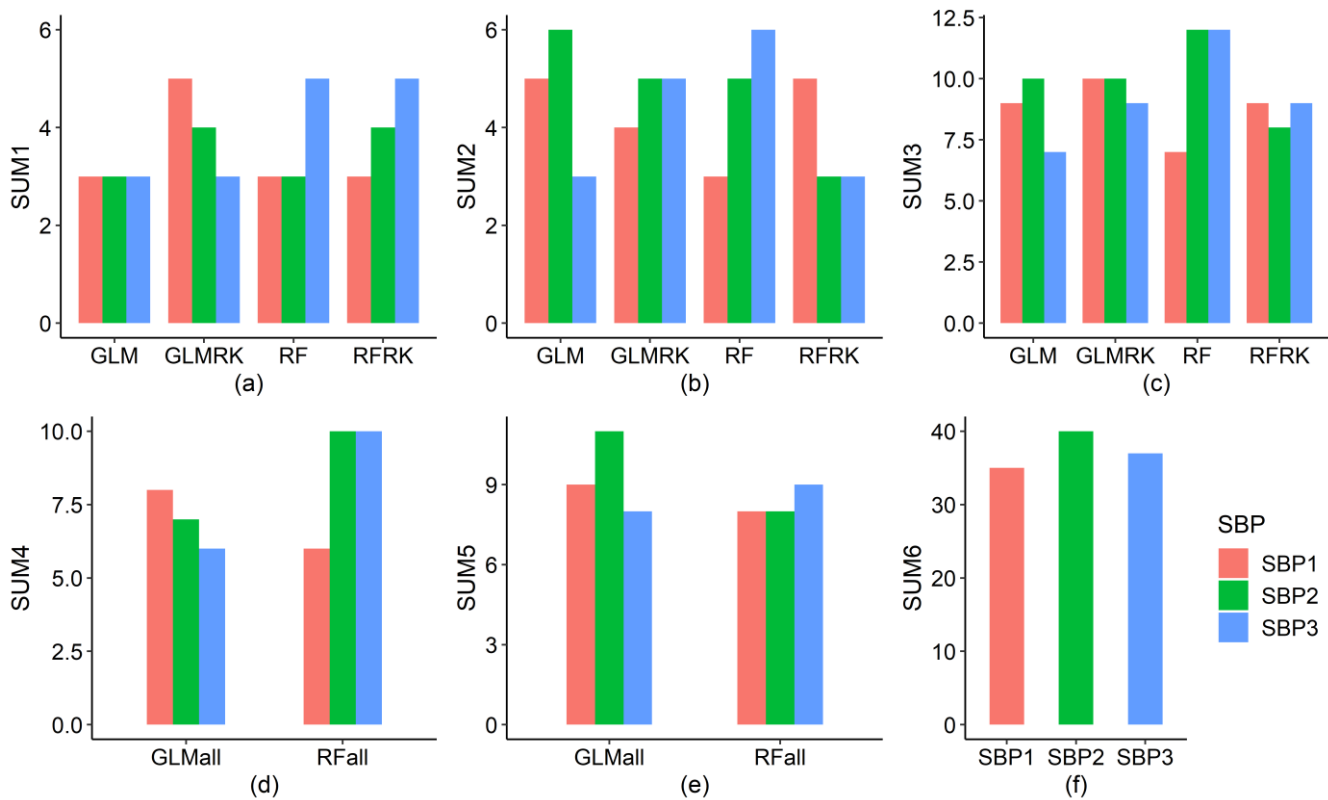
5 *"**Figure 5.** Ranking score of model performance based on three SBPs. SUM1 (a) and SUM2 (b) are the sum scores of ME and RMSE for each model, respectively. SUM3 (c) is the sum score of ME, RMSE, and AD for each model; SUM4 (d) and SUM5 (e) are the sum scores of ME or RMSE for GLM_all (GLM and GLMRK) and RF_all (RF and RFRK); SUM6 (f) is the sum score of all indicators. The lower the value of these scores, the better the model performance."*

10 **P20L415:** *"The three SBP-based datasets generated different distributions; a statistical significance test proved that most models had significant differences in prediction accuracy using different SBPs. A ranking score was provided to demonstrate these differences, and compositional balance should be considered when mapping soil PSFs."*

Reference

Diebold, F.X. and Mariano, R.S.: Comparing predictive accuracy. Journal of Business and Economic Statistics, 13, 253-263,
15   1995.

Harvey, D., Leybourne, S., and Newbold, P.: Testing the equality of prediction mean squared errors. International Journal of
     forecasting, 13(2), 281-291, 1997.

Table S6.1. The statistical significance *p*-value (Diebold-Mariano test) of predicted ME of sand fractions among different models.

ME_Sand	GLM_SB P1	GLM_SB P2	GLM_SB P3	GLMRK_SB P1	GLMRK_SB P2	GLMRK_SB P3	RF_SBP 1	RF_SBP 2	RF_SBP 3	RFRK_SB P1	RFRK_SB P2	RFRK_SB P3
GLM_SBP1	-											
GLM_SBP2	0.07	-										
GLM_SBP3	0.85	0.22	-									
GLMRK_SB P1	0.83	0.19	0.98	-								
GLMRK_SB P2	0.18	0.67	0.20	0.02**	-							
GLMRK_SB P3	0.84	0.31	0.90	0.89	0.03**	-						
RF_SBP1	0.06	0.61	0.04**	0.08	0.89	0.15	-					
RF_SBP2	0.02**	0.39	0.02**	0.04**	0.71	0.12	0.25	-				
RF_SBP3	0.02**	0.35	0.02**	0.03**	0.61	0.09	0.08	0.41	-			
RFRK_SBP1	0.39	0.90	0.38	0.39	0.93	0.46	0.83	0.70	0.63	-		
RFRK_SBP2	0.28	0.71	0.28	0.30	0.89	0.37	0.95	0.92	0.84	0.20	-	
RFRK_SBP3	0.33	0.76	0.32	0.32	0.93	0.39	0.99	0.88	0.81	0.29	0.72	-

*Note that $p>0.05$: not significant; $0.01<p<0.05$: significant; $p<0.01$: highly significant. The null hypothesis is that the two methods have the same level of prediction accuracy, and the alternative hypothesis is that method 1 and method 2 have different levels of accuracy (when $p<0.05$, null hypothesis rejected).

Table S6.2. The statistical significance *p*-value (Diebold-Mariano test) of predicted ME of silt fractions among different models.

ME_Silt	GLM_SB P1	GLM_SB P2	GLM_SB P3	GLMRK_SB P1	GLMRK_SB P2	GLMRK_SB P3	RF_SBP 1	RF_SBP 2	RF_SBP 3	RFRK_SB P1	RFRK_SB P2	RFRK_SB P3
GLM_SBP1	-											
GLM_SBP2	0.32	-										
GLM_SBP3	0.72	0.63	-									
GLMRK_SB P1	0.03**	0***	0.01**	-								
GLMRK_SB P2	0.40	0.07	0.23	0.16	-							
GLMRK_SB P3	0.19	0.04**	0.05	0.83	0.19	-						
RF_SBP1	0***	0***	0***	0***	0***	0***	-					
RF_SBP2	0***	0***	0***	0***	0***	0***	0.01**	-				
RF_SBP3	0***	0***	0***	0***	0***	0***	0***	0.67	-			
RFRK_SBP1	0.01**	0.02***	0.01**	0***	0***	0***	0.44	0.23	0.20	-		
RFRK_SBP2	0.01**	0.01**	0.01**	0***	0***	0***	0.72	0.44	0.39	0.12	-	
RFRK_SBP3	0.01**	0.01**	0***	0***	0***	0***	0.85	0.54	0.49	0.03**	0.36	-

*Note that $p>0.05$: not significant; $0.01<p<0.05$: significant; $p<0.01$: highly significant. The null hypothesis is that the two methods have the same level of prediction accuracy, and the alternative hypothesis is that method 1 and method 2 have different levels of accuracy (when $p<0.05$, null hypothesis rejected).

Table S6.3. The statistical significance p-value (Diebold-Mariano test) of predicted ME of clay fractions among different models.

ME_Clay	GLM_SB P1	GLM_SB P2	GLM_SB P3	GLMRK_SB P1	GLMRK_SB P2	GLMRK_SB P3	RF_SBP 1	RF_SBP 2	RF_SBP 3	RFRK_SB P1	RFRK_SB P2	RFRK_SB P3
GLM_SBP1	-											
GLM_SBP2	0.06	-										
GLM_SBP3	0.07	0.95	-									
GLMRK_SB P1	0***	0***	0***	-								
GLMRK_SB P2	0.02**	0***	0***	0.39	-							
GLMRK_SB P3	0.04**	0***	0***	0.12	0.55	-						
RF_SBP1	0***	0***	0***	0***	0***	0***	-					
RF_SBP2	0***	0***	0***	0***	0***	0***	0.04**	-				
RF_SBP3	0***	0***	0***	0***	0***	0***	0.04**	0.64	-			
RFRK_SBP1	0.03**	0.15	0.11	0***	0***	0***	0.36	0.26	0.28	-		
RFRK_SBP2	0.03**	0.14	0.11	0***	0***	0***	0.35	0.26	0.27	0.97	-	
RFRK_SBP3	0.02**	0.09	0.07	0***	0***	0***	0.56	0.43	0.45	0.01**	0.01**	-

*Note that $p>0.05$: not significant; $0.01<p<0.05$: significant; $p<0.01$: highly significant. The null hypothesis is that the two methods have the same level of prediction accuracy, and the alternative

hypothesis is that method 1 and method 2 have different levels of accuracy (when p<0.05, null hypothesis rejected).

Table S6.4. The statistical significance *p*-value (Diebold-Mariano test) of predicted RMSE of sand fractions among different models.

RMSE_Sand	GLM_SBP 1	GLM_SBP 2	GLM_SBP 3	GLMRK_SBP 1	GLMRK_SBP 2	GLMRK_SBP 3	RF_SBP 1	RF_SBP 2	RF_SBP 3	RFRK_SBP 1	RFRK_SBP 2	RFRK_SBP 3
GLM_SBP1	-											
GLM_SBP2	0***	-										
GLM_SBP3	0.42	0.02**	-									
GLMRK_SBP 1	0.02**	0***	0.01**	-								
GLMRK_SBP 2	0.03**	0.07	0.18	0***	-							
GLMRK_SBP 3	0.94	0.02**	0.53	0.01	0.08	-						
RF_SBP1	0.01**	0***	0.01**	0.77	0***	0.1	-					
RF_SBP2	0.02**	0***	0.01**	0.76	0***	0.09	0.92	-				
RF_SBP3	0.07	0***	0.04**	0.88	0.01**	0.22	0***	0.01**	-			
RFRK_SBP1	0.16	0***	0.12	0.61	0.02**	0.19	0.72	0.72	0.54	-		
RFRK_SBP2	0.26	0.01**	0.19	0.79	0.03**	0.28	0.92	0.92	0.72	0.05**	-	
RFRK_SBP3	0.23	0.01**	0.16	0.74	0.03**	0.25	0.87	0.88	0.67	0.08	0.61	-

*Note that $p>0.05$: not significant; $0.01<p<0.05$: significant; $p<0.01$: highly significant. The null hypothesis is that the two methods have the same level of prediction accuracy, and the alternative hypothesis is that method 1 and method 2 have different levels of accuracy (when $p<0.05$, null hypothesis rejected).

Table S6.5. The statistical significance *p*-value (Diebold-Mariano test) of predicted RMSE of silt fractions among different models.

RMSE_Silt	GLM_SB P1	GLM_SB P2	GLM_SB P3	GLMRK_SB P1	GLMRK_SB P2	GLMRK_SB P3	RF_SBP 1	RF_SBP 2	RF_SBP 3	RFRK_SB P1	RFRK_SB P2	RFRK_SB P3
GLM_SBP1	-											
GLM_SBP2	0.44	-										
GLM_SBP3	0.03**	0.01**	-									
GLMRK_SB P1	0.01**	0.01**	0.98	-								
GLMRK_SB P2	0.50	0.80	0.02**	0***	-							
GLMRK_SB P3	0.24	0.12	0.70	0.67	0.02	-						
RF_SBP1	0***	0***	0***	0***	0***	0***	-					
RF_SBP2	0***	0***	0***	0***	0***	0***	0***	-				
RF_SBP3	0***	0***	0***	0***	0***	0.01**	0***	0.01	-			
RFRK_SBP1	0***	0***	0***	0***	0***	0***	0.27	0.10	0.05**	-		
RFRK_SBP2	0***	0***	0***	0***	0***	0***	0.69	0.36	0.23	0***	-	
RFRK_SBP3	0***	0***	0***	0***	0***	0***	0.54	0.24	0.14	0.01**	0.36	-

*Note that $p>0.05$: not significant; $0.01<p<0.05$: significant; $p<0.01$: highly significant. The null hypothesis is that the two methods have the same level of prediction accuracy, and the alternative

hypothesis is that method 1 and method 2 have different levels of accuracy (when p<0.05, null hypothesis rejected).

Table S6.6. The statistical significance *p*-value (Diebold-Mariano test) of predicted RMSE of clay fractions among different models.

RMSE_Clay	GLM_SB P1	GLM_SB P2	GLM_SB P3	GLMRK_SB P1	GLMRK_SB P2	GLMRK_SB P3	RF_SBP 1	RF_SBP 2	RF_SBP 3	RFRK_SB P1	RFRK_SB P2	RFRK_SB P3
GLM_SBP1	-											
GLM_SBP2	0.05**	-										
GLM_SBP3	0.02**	0.45	-									
GLMRK_SB P1	0.32	0.05**	0.01**	-								
GLMRK_SB P2	0.50	0.65	0.34	0.01**	-							
GLMRK_SB P3	0.84	0.39	0.16	0.66	0.42	-						
RF_SBP1	0***	0***	0***	0***	0***	0***	-					
RF_SBP2	0***	0***	0***	0***	0***	0***	0***	-				
RF_SBP3	0***	0***	0***	0***	0***	0***	0.84	0***	-			
RFRK_SBP1	0***	0***	0***	0***	0***	0***	0.74	0.29	0.72	-		
RFRK_SBP2	0***	0***	0***	0***	0***	0***	0.67	0.27	0.66	0.59	-	
RFRK_SBP3	0***	0***	0***	0***	0***	0***	0.63	0.23	0.60	0.50	0.87	-

*Note that $p>0.05$: not significant; $0.01<p<0.05$: significant; $p<0.01$: highly significant. The null hypothesis is that the two methods have the same level of prediction accuracy, and the alternative hypothesis is that method 1 and method 2 have different levels of accuracy (when $p<0.05$, null hypothesis rejected).

Table S6.7. The statistical significance *p*-value (Diebold-Mariano test) of predicted AD among different models.

AD	GLM_SB P1	GLM_SB P2	GLM_SB P3	GLMRK_SB P1	GLMRK_SB P2	GLMRK_SB P3	RF_SBP 1	RF_SBP 2	RF_SBP 3	RFRK_SB P1	RFRK_SB P2	RFRK_SB P3
GLM_SBP1	-											
GLM_SBP2	0.92	-										
GLM_SBP3	0.08	0.08	-									
GLMRK_SB P1	0.63	0.70	0.41	-								
GLMRK_SB P2	0.97	0.98	0.25	0.31	-							
GLMRK_SB P3	0.77	0.81	0.42	0.95	0.70	-						
RF_SBP1	0***	0***	0***	0***	0***	0***	-					
RF_SBP2	0***	0***	0***	0***	0***	0***	0***	-				
RF_SBP3	0***	0***	0***	0***	0***	0***	0.06	0.2	-			
RFRK_SBP1	0***	0***	0***	0***	0***	0***	0.28	0.12	0.17	-		
RFRK_SBP2	0***	0***	0***	0***	0***	0***	0.38	0.17	0.23	0.34	-	
RFRK_SBP3	0***	0***	0***	0***	0***	0***	0.38	0.18	0.23	0.32	0.95	-

*Note that $p>0.05$: not significant; $0.01<p<0.05$: significant; $p<0.01$: highly significant. The null hypothesis is that the two methods have the same level of prediction accuracy, and the alternative hypothesis is that method 1 and method 2 have different levels of accuracy (when $p<0.05$, null hypothesis rejected).

X

5

Comment 5: The authors should carefully check the English for grammar errors throughout the manuscript. A serious editing and proof-reading are required.

Response: Thanks for the referee's suggestion about the English quality of this paper. We looked for some senior editors from a professional English polishing company to improve the overall language of this article and we have checked and improved the writing in the revised version. The editorial certificate is shown as follows:

Charlesworth
Author Services

EDITORIAL CERTIFICATE

This document certifies that the manuscript below was edited for correct English language usage, grammar, punctuation and spelling by qualified native English speaking editors at Charlesworth Author Services.

Paper Title:

Compositional balance should be considered in soil particle-size fractions mapping using hybrid interpolators

Author:

Wenjiao Shi

Date certificate issued:

August 16, 2021

cwauthors.com

Compositional balance should be considered in the mapping of soil particle-size fractions using hybrid interpolators

Mo Zhang[1,2], Wenjiao Shi[1,~~3~~2]

[1]Key Laboratory of Land Surface Pattern and Simulation, <u>State Key Laboratory of Resources and Environmental Information System,</u> Institute of Geographic Sciences and Natural Resources Research, Chinese Academy of Sciences, Beijing 100101, China
[2]~~School of Earth Sciences and Resources, China University of Geosciences, Beijing 100083, China~~
[~~3~~2]College of Resources and Environment, University of Chinese Academy of Sciences, Beijing 100049, China

Correspondence to: Wenjiao Shi (<u>shiwj@lreis.ac.cn</u>), Institute of Geographic Sciences and Natural Resources Research, Chinese Academy of Sciences. 11A, Datun Road, Chaoyang District, Beijing 100101, China.

Abstract. Digital soil mapping of soil particle-size fractions (PSFs) using log-ratio methods is a widely used technique. As a hybrid interpolator, regression kriging (RK) is ~~an alternative~~one way to improve prediction accuracy <u>of soil PSFs</u>. However, there is still a lack of comparisons and recommendations when RK is applied for compositional data~~, and it~~. It is ~~not known~~unknown if the <u>prediction</u> performance based on different balances of <u>the</u> isometric log-ratio (ILR) transformation is robust. ~~Here, we~~We compared the generalized linear model (GLM), <u>the</u> random forest (RF~~),~~) model, and their hybrid patterns (~~RK~~<u>i.e., GLMRK and RFRK</u>) using different transformed data based on three ILR balances~~, with~~. <u>The comparison involved</u> 29 environmental covariables ~~(ECs)~~ for the ~~prediction of~~ soil ~~PSFs~~<u>PSF prediction</u> in the upper reaches of the Heihe River Basin, China. The results showed that RF performed best, with more accurate predictions, but GLM produced a more unbiased prediction. For the hybrid interpolators, RK was recommended because it widened the data ranges of the prediction values~~,~~ and modified the bias and accuracy for most models, especially for RF. Moreover, prediction maps generated from RK revealed more details of the soil sampling points. For three ILR balances, different data distributions were produced. Using the most abundant component of the compositional data as the first component of the permutations was not considered the ~~right~~best choice ~~because it produced the worst performance~~<u>for soil PSF mapping</u>. Compared to the relative abundance of components, we recommend that the focus should be on data distribution. This study provides a reference for ~~the~~ mapping ~~of~~ soil PSFs combined with transformed data at the regional scale.

1 Introduction

Recently, spatial interpolation of soil particle-size fractions (PSFs) has become a focus of soil science researchers. More accurately predicted soil PSFs ~~could contribute to a better understanding of~~elucidates hydrological, physical, and environmental processes (Delbari et al., 2011; Ließ et al., 2012; McBratney et al., 2002).

The characteristics of compositional data ~~makes~~make soil PSFs more impressive than other soil properties. Soil PSFs are

usually expressed as three components ~~of~~for discrete data—— sand, silt, and clay~~, —~~ and carry only relevant percentage information. Soil texture is classified ~~as~~by soil PSFs, which can be demonstrated on a ternary diagram (so-called soil texture triangle). ~~The~~However, the closure system formed in this triangle is not in Euclidean space, but ~~is~~rather Aitchison space (i.e., ~~the~~a simplex) (Aitchison, 1986). Due to "spurious correlations" (Pawlowsky-Glahn, 1984), traditional statistical methods based on ~~the~~Euclidean geometry may generate mistakes when dealing directly with soil PSF data (Filzmoser et al., 2009). The requirement for constant-_sum, nonnegative, unbiased prediction is the key to spatial interpolation (Walvoort and de Gruijter, 2001). ~~Data~~Therefore, data transformation from a simplex into real space is crucial for compositional data ~~from the simplex to the real space~~. Log ratio transformations play a significant role in compositional data analysis, including the additive log-ratio (ALR), centered log-ratio (CLR) (Aitchison, 1986), and the isometric log-ratio (ILR) (Egozcue et al., 2003).

Although these three log-ratio methods have been widely applied to transform soil PSF data, different study area scales and model selection should be considered when modeling. For local-_scale study areas, geostatistical models~~, i.e., ordinary kriging (OK) and compositional kriging,~~ combined with log-ratio transformed data~~,~~ are sufficient to map spatial patterns, as shown in our previous study (Wang and Shi, 2017). ~~As~~From another perspective, functional compositions combined with the kriging method can also be applied to produce soil particle size curves (PSCs) (Menafoglio et al., 2014), providing an abundance of information. ~~This involves~~Functional compositions involve the use of complete and continuous information rather than discrete information, and soil PSFs can be extracted from the predicted soil PSCs (Menafoglio et al., 2016a). Log-ratio transformations can also be combined with functional-compositional data for the stochastic simulation of PSCs (Menafoglio et al., 2016b, Talska et al., 2018). For middle-_scale study areas, outliers may lead to ~~the~~overestimation of the variogram, resulting in prediction errors (Lark, 2000). Therefore,~~ the~~ spatial interpolation should take robust variogram estimators into account to improve model performance (Lark, 2003). A previous study proved that applying robust variogram estimators in log-ratio co-kriging significantly improved mapping performance (Wang and Shi, 2018). For large-_scale study areas, geostatistical models are limited by the number of soil samples and increased spatial variability. ~~An increasing number~~Increasing numbers of studies have concentrated on mapping soil PSFs using different machine-learning models combined with ancillary data (i.e., environmental covariables, ECs~~)~~). Log-ratio transformed data have been applied on a broad basin scale (Zhang et al., 2020), national scale (Akpa et al., 2014), and even a global scale (Hengl et al., 2017~~) using log-ratio transformed data.~~).

Among these EC-combined models, linear, machine-learning, geostatistical models, and high-_accuracy surface modeling (Yue et al., 2020; Shi et al., 2016) have been commonly used in middle or large-scale studies. Linear models, for example, the generalized linear model (GLM) and multiple linear regression (MLR) model, have been used in soil PSF predictions ~~with~~because of their flexibility and interpretability (Lane, 2002; Buchanan et al., 2012). Many machine-learning models have been applied for ~~the~~soil PSF interpolation and soil texture classification. For example, tree learners, such as the random forest (RF~~), have been shown to be~~) model, are advantageous due to their ability to handle overfitting and generate more realistic maps (Zhang et al., 2020). ~~Furthermore~~In addition, regression kriging (RK~~), which~~) has ~~been proved~~proven to be a powerful

74 and widely accepted method ~~of~~for soil ~~mapping, can not only combine~~interpolation. ECs can be introduced through its

75 regression function~~, but it also improves~~ and improved model accuracy as a hybrid interpolator for some soil properties, such

76 as topsoil thickness and pH (Hengl et al., 2004; Keskin and Grunwald, 2018; Shi et al., 2009; Shi et al., 2011). However, the

77 scope of the comparison needs to be expanded to further explore the prediction accuracy ~~and predict~~combined with

78 compositional data using linear models, machine-learning models, and combining RK with other models ~~combining RK~~

79 (hybrid patterns).

80 In log-ratio methods, the ILR method performs better than the ALR and CLR methods in both theory and ~~in~~ practice

81 (Filzmoser and Hron, 2009; Wang and Shi, 2018; Zhang et al., 2020). The ILR method eliminates model collinearity and

82 preserves advantageous properties~~.~~, such as isometry, scale invariance, and sub-compositional coherence~~, through its use of~~.

83 The ILR method is constructed in orthonormal coordinate systems (i.e., balances) using a sequential binary partition (SBP)

84 (Egozcue and Pawlowsky-Glahn, 2005). ~~These~~The choices of balances are not unique~~, multiple~~. Multiple sets of ILR

85 transformed data can be generated by permutations of components (different SBPs) in the compositional data. The

86 ~~choice~~selection of an SBP can be based on prior expert knowledge, using a compositional biplot (Lloyd et al., 2012) or

87 variograms and cross-variograms (Molayemat et al., 2018). It has been proven in statistical science that different results are

88 obtained using different ~~choices of ILR balances, and~~ILR balances. For example, Fiserova and Hron (2011) reported that

89 different balances generated different covariance structures. Moreover, the choice of SBP is related to hypotheses, research

90 questions of interest, or the context of the data analysis (Coenders et al., 2017; Facevicova et al., 2018). Thus, the option of a

91 specific SBP for compositions is crucial for the intended interpretation of coordinates (Fiserova and Hron, 2011). However,

92 most soil science researchers have ignored this point. Martins et al. (2016) reported that clay ~~has been~~was used as the

93 denominator in the ALR method because it is typically the most abundant component of compositions. Few studies have

94 compared and analyzed the different SBP options from the perspective of accurate ~~assessments~~assessment and ~~analyzed~~

95 whether these differences are due to the general characteristics of specific data sets or log-ratio transformations.

96 Therefore, based on our previous work, the objectives of this study were to: (i) compare the spatial prediction accuracy of

97 soil PSFs using a GLM and RF method combined with ECs and ILR transformed data; (ii) determine whether hybrid

98 interpolators (GLMRK and RFRK) can improve the ~~interpolation performance~~prediction accuracy; and (iii) explore the

99 distributions of different transformed data and the variation law of precision based on different choices of SBP.

2 Methods and materials

2.1 Study area

102 The study area was the upper reaches of the Heihe River Basin (HRB), which is the source of the Heihe River and the central

103 area of runoff generation in the HRB. The elevation in this area ranges from 1640 to 5573 m (Fig. 1), and the climate is damp

104 and cold, due to the area being dominated by the Qilian Mountains. The mean annual rainfall in the study area is 350 mm, and

105 the mean annual temperature is lower than 4°C. Meadow and steppe are the dominant vegetation types. Grassland is the

106 primary land-use type. The main soil classes are frigid calcic soil in the southwest of the study area, with cold desert soil

107 dominating the southeast, while Castanozems and Sierozems are distributed in the north of the study area.
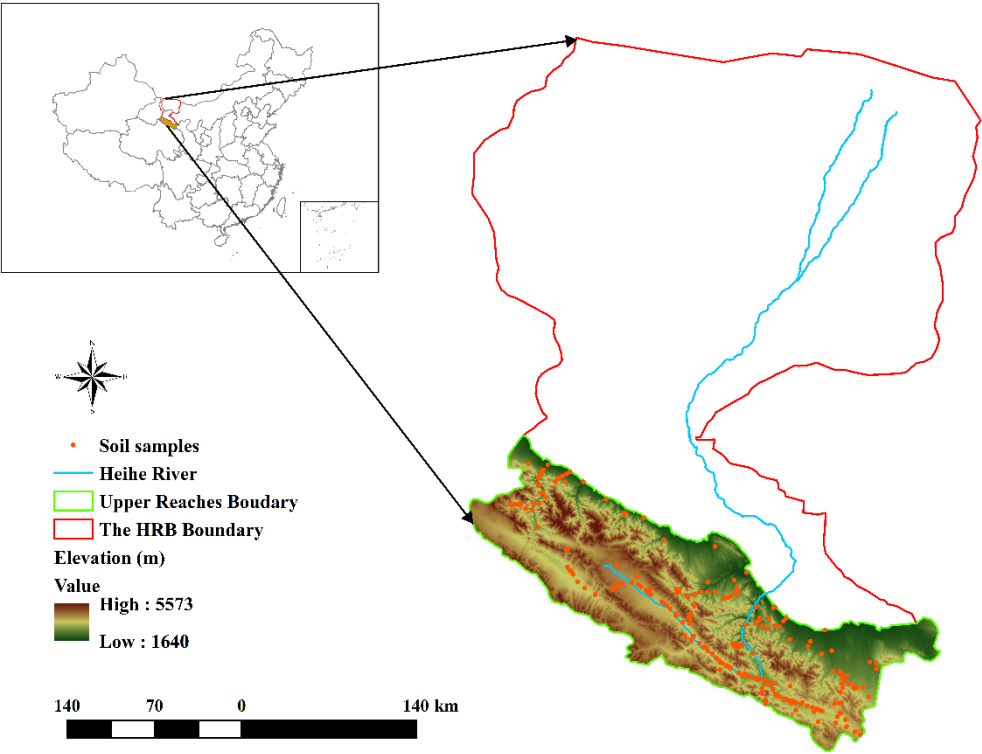

108

109 **Figure. 1.** ~~The location~~Location, elevation, and soil samples on the upper reaches of the Heihe River Basin.

110 **2.2 Data collection and analysis**

111 **2.2.1 Soil PSF data**

112 A total of 262 soil samples were collected in the upper reaches of the HRB based on a purposive sampling strategy and were

113 used to characterize the spatial variability of soil PSFs at the regional scale (Fig. 1). The variability of soil formation factors,

114 such as elevation, soil type, vegetation class, and geomorphology of the upper reaches of the HRB, was considered in soil

115 sample collection. ~~The~~An average of three mixed topsoil samples (approximate depth of 0–20 cm) was obtained to reduce the

116 noise of soil sample parameters, and a parallel sample was also measured. Subsequently, about 30 g of each soil sample was

117 air-dried, and chemical and physical analyses were conducted in the laboratory. Soil PSF information was obtained ~~for~~from

118 the soil samples using a Malvern Panalytical Mastersizer 2000, with less than a 3% average measurement error.

4

2.2.2 The selection of ECs

There were 29 ECs considered in our study after reducing the level of correlation between the variables, including both continuous and categorical variables (Table S1.1). ~~They~~These ECs followed the principles of the SCORPAN model (McBratney et al., 2003). The continuous variables included the morphometry and hydrologic characteristics of topographic properties, climatic and vegetative indices, and soil physical and chemical properties (Yi et al., 2015; Song et al., 2016; Yang et al., 2016). The categorical variables included geomorphology, land use types, and vegetation classes, which were transformed into ~~raster~~rasters with 1000 m resolution. Due to the intricate patterns of topography in the upper reaches of the HRB, the variable of topographic properties ~~dominated~~dominate the ECs. The System for Automated Geoscientific Analyses geographic information system (SAGA GIS, Conrad et al., 2015) was applied for a terrain analysis to derive topographic variables using the 30 m resolution digital elevation model (DEM, http://www.gscloud.cn). A collinearity test removed the redundant variables, and the topographic properties were then resampled to 1000 m. More details of the ECs are provided in the Data Availability section.

2.3 ILR transformation and SBP

An orthonormal basis of ILR was chosen to isometrically project the compositions from S^D (the simplex for the Aitchison geometry) to R^{D-1} (real space for the Euclidean geometry). The choice of a specific orthonormal basis for use on S^D can be explained by the SBP for the groups of compositions (Egozcue and Pawlowsky-Glahn, 2005). The choice of the construction of coordinates (i.e., balances) between groups of compositions was calculated as follows:

$$z_k = \sqrt{\frac{r_k s_k}{r_k + s_k}} \ln\left(\frac{(x_{i_1} x_{i_2} \dots x_{i_{r_k}})^{1/r_k}}{(x_{j_1} x_{j_2} \dots x_{j_{s_k}})^{1/s_k}}\right), \ k = 1, \dots, D-1,$$

$$\tag{1}$$

where z_k refers to the balance between two groups; $i_1, i_2, \dots, i_{r_k}$ is the r_k part of one group; and $j_1, j_2, \dots, j_{r_k}$ is the s_k part of the other group. Therefore, in a stepwise manner, the balances contain all the relevant information of the compositions in two groups. This can also be ~~explained~~displayed in ~~a~~ tabular form. For soil PSF data (D = 3), all three choices of the balance of SBPs are shown in Table 1. The first component of the ILR contained all the information on soil PSFs, and the main difference in the choice of balances for soil PSFs was the order of the three parts~~,~~; i.e., the first order of the soil PSF component was used as the numerator of the first ILR equation. In our study, three SBP balances, SBP1, SBP2, and SBP3, were transformed from the original soil PSF data, and the orders of soil PSF data were $(sand, silt, clay)$, $(silt, clay, sand)$, and $(clay, sand, silt)$, respectively. The transformation equations for the ILR can be derived from Eq. (1), and ~~were defined as~~constitute Eqs. (2) and (3). The inverse equations for ILR ~~were defined as~~constitute Eqs. (4)~~, (5),~~ – (6). The ILR transformation and its inverse were conducted using the R package "compositions" (K. Gerald ~~van den Boogaart and Raimon Tolosana,~~et al., 2014).

5

149    $\mathbf{z} = (z_1, \ldots z_{D-1}) = ILR(\mathbf{x})$, and for $i = 1, \ldots, D-1$ and component x_i,

150   (2)

151    $z_i = \sqrt{\dfrac{D-i}{D-i+1}} \ln \dfrac{x_i}{\sqrt[D-i]{\prod_{j=i+1}^{D} x_j}}.$

152   (3)

153    $Y(x_j) = \sum_{j=1}^{D} \dfrac{ILR(x_j)}{\sqrt{j \times (j+1)}} - \sqrt{\dfrac{j-1}{j}} \times ILR(x_j),$ (4)

154    $ILR(x_0) = ILR(x_D) = 0,$ (5)

155    $\overline{ILR}(x_j) = \dfrac{exp(Y(x_j))}{\sum_{j=1}^{D} exp(Y(x_j))}.$ (6)

156 **Table 1.** All choices of SBPs for soil PSF data (D = 3); the order of soil PSFs data is $(sand, silt, clay)$,

157 $(silt, clay, sand)$, and $(clay, sand, silt)$ for SBP1, SBP2 and SBP3.

Groups	Step	Sand	Silt	Clay	r	s	Balance
SBP1	1	+	-	-	1	2	Step1: $z_1 = \sqrt{\frac{2}{3}} \ln \frac{sand}{\sqrt{silt \times clay}}$
	2	0	+	-	1	1	Step2: $z_2 = \sqrt{\frac{1}{2}} \ln \frac{silt}{clay}$
SBP2	1	-	+	-	1	2	Step1: $z_1 = \sqrt{\frac{2}{3}} \ln \frac{silt}{\sqrt{clay \times sand}}$
	2	-	0	+	1	1	Step2: $z_2 = \sqrt{\frac{1}{2}} \ln \frac{clay}{sand}$
SBP3	1	-	-	+	1	2	Step1: $z_1 = \sqrt{\frac{2}{3}} \ln \frac{clay}{\sqrt{sand \times silt}}$
	2	+	-	0	1	1	Step2: $z_2 = \sqrt{\frac{1}{2}} \ln \frac{sand}{silt}$

158

159 **2.4 Linear model, machine-learning model, and hybrid patterns**

160 **2.4.1 GLM**

161 The GLM is an extended version of the linear model, which contains response variables with non-normal distributions (Nelder

162 and Wedderburn, 1972). The link function is embedded into the GLM to ensure that classical linear model assumptions are

163 met. The scaled dependent variables and the independent variables can be connected using a link function for the additive

164 combination of model effects; the choice of link function depends on the distribution of response variables (Venables and

165 Dichmont, 2004). A Gaussian distribution with an identity link function was applied in our study, which produced

6

166 consequences equivalent to ~~that~~those of the MLR (Nickel et al., 2014). However, categorical variables can be directly trained

167 in the GLM without setting dummy variables. The Akaike's information criterion (AIC) was applied to choose the best

168 predictors and remove model multicollinearity using a backward stepwise algorithm, and the combinations of ECs for different

169 ILR data were then obtained (Table S2.1).

170 **2.4.2 RF**

171 The RF is a non-parametric technique, which combines the bagging method with a selection of random variables as an extended

172 version of a regression tree (RT) (Breiman, 1996, 2001). It can improve model prediction accuracy by producing and

173 aggregating multiple tree models. The principle of the RF is to merge a group of "weak trees" together to generate a "powerful

174 forest." The bootstrap sampling method was applied for each tree, and each predictor was selected randomly from all model

175 predictors. The "out of bag" (OOB) data were applied to produce reliable estimates in an internal validation using a random

176 subset independent of the training tree data. Three parameters needed to be tuned: the number of trees ($ntree$~~;~~), minimum

177 size of terminal nodes ($nodesize$), and the number of variables randomly sampled as predictors for each tree ($mtry$) (Liaw

178 and Wiener, 2001). The standard value of the $mtry$ parameter was one-third of the total number of predictors, while $ntree$

179 and $nodesize$ were 500 and 5, respectively. For regression, the mean square errors (MSEs) of predictions were estimated to

180 train the trees. The variable importance of the RF was produced from the OOB data using the "importance" function. One of

181 the benefits of the RF is that ~~the~~ ensembles of trees are used without pruning to ensure that the most significant amount of

182 variance can be expressed. Moreover, the RF can reduce model overfitting, and normalization is unnecessary due to the effects

183 on the value range being ~~insensitive~~slight. The GLM and RF algorithms and the parameter adjustment of the RF were

184 conducted in the R package "caret" (Max Kuhn, 2018).

185

186 **2.4.3 RK**

187 Regression kriging is a hybrid interpolation technique that combines regression models (e.g., GLM and RF) with the residuals

188 of ordinary kriging (OK~~(,~~ Odeh et al., 1995). Mathematically, the RK method corresponds to two interpolators, the regression

189 part and the kriging part, which are operated separately (Goovaerts, 1999). One limitation of using only the regression part is

190 that it is usually only useful within the range of values of the training sets (Hengl et al., 2015). The principle of the RK method

191 is that the regression model explains a deterministic component of spatial variability, and the interpolation of regression

192 residuals generated from OK is used to describe the spatial variability (Bishop and McBratney, 2001; Hengl et al., 2004). The

193 residuals create a variogram (e.g., Gaussian, spherical, or exponential) for models based on the MSE from the results of a

194 cross-validation. First, we used the regression part (GLM or RF) to predict soil PSFs~~, the~~. The residual from the fitted model

195 was then calculated by subtracting the regression part from the observations. Subsequently, OK was applied ~~for~~to the whole

196 study area to interpolate the residuals. Finally, the regression ~~prediction~~predictions and the predicted residuals at the same

location were summed. The variograms of the RK method were generated automatically using the "autofitVariogram" function in the R package "automap" (Hiemstra et al., 2009). Details of the of RK method in our study can be found in the Supplementary Material Section S6.

2.5 Prediction method system and validation

The method ~~system~~ of spatial interpolation ~~models~~ for soil PSFs is presented in Table 2. We systematically compared 12 models: the combinations of four interpolators ~~, including~~ (GLM ~~and~~, GLMRK, RF ~~with or without RK~~, RFRK), and three SBPs of the ILR transformation method. For the validation of model performance, ~~the~~ independent data set validation was used to evaluate the prediction bias and accuracy of the models. The ~~sub-~~ data were randomly divided into two sets: the sub-training sets (70%) and the sub-testing sets (30~~%) were randomly selected from data independently,~~%), and this process was repeated 30 times. Moreover, the Diebold–Mariano test (Diebold and Mariano, 1995; Harvey et al., 1997) was used to verify the statistical significance of the differences among the models.

Table 2. The method ~~system~~ of spatial interpolation ~~models~~ of soil PSFs.

Models	GLM	GLMRK	RF	RFRK
~~ILR~~ SBP1	GLM_SBP1	GLMRK_SBP1	RF_SBP1	RFRK_SBP1
~~ILR~~ SBP2	GLM_SBP2	GLMRK_SBP2	RF_SBP2	RFRK_SBP2
~~ILR~~ SBP3	GLM_SBP3	GLMRK_SBP3	RF_SBP3	RFRK_SBP3

The mean error (ME), the root mean square error (RMSE), and Aitchison distance (AD) were used to evaluate and compare the prediction performance. The ME and RMSE measure prediction bias and accuracy, respectively (Odeh et al., 1995). The AD is an overall indicator of compositional analysis, which describes the distance between two compositions. Generally, in an accurate, unbiased model all three values will be close to 0. The ranges of a 95% confidence interval (CI) (Streiner, 1996) of ME, RMSE, and AD were calculated to compare the uncertainties of different models. The ME, RMSE, and AD were calculated as follows:

$$ME = \frac{1}{n}\sum_{i=1}^{n}(M_i - P_i), \tag{7}$$

$$RMSE = \sqrt{\frac{1}{n}\sum_{i=1}^{n}(M_i - P_i)^2}, \tag{8}$$

$$AD = \left[\sum_{i=1}^{D}\left(log\frac{M_i}{G(M)} - log\frac{P_i}{G(P)}\right)^2\right]^{0.5}, \tag{9}$$

where M_i and P_i are the measured and predicted values ~~at~~of the ith ~~position, respectively~~sample for sand, silt and clay; n refers to the number of soil samples; D is the number of dimensions of compositions; and $G(\boldsymbol{M})$ and $G(\boldsymbol{P})$ denote the geometric mean with the form $G(\mathbf{x}) = (x_1, \ldots, x_D)^{1/D}$ of the measured and predicted values, respectively.

2.6 Covariance structure analysis

The interpretation of the ILR balances is based on a decomposition of the covariance (COV) structure (Fiserova and Hron, 2011). We calculated the variance (VAR), COV, and the corresponding correlation coefficient (CC) of ILR transformed data based on different ~~SBP~~SBPs. The equations for calculating VAR, COV, and CC were derived from Eq. (1) as follows:

$$VAR(z) = \frac{1}{r+s}\sum_{p=1}^{r}\sum_{q=1}^{s}var\left(ln\frac{x_{i_p}}{x_{j_q}}\right) - \frac{s}{2r(r+s)}\sum_{p=1}^{r}\sum_{q=1}^{r}var\left(ln\frac{x_{i_p}}{x_{i_q}}\right) - \frac{r}{2s(r+s)}\sum_{p=1}^{s}\sum_{q=1}^{s}var\left(ln\frac{x_{j_p}}{x_{j_q}}\right) -$$

$$\frac{r}{2s(r+s)}\sum_{p=1}^{s}\sum_{q=1}^{s}var\left(ln\frac{x_{j_p}}{x_{j_q}}\right) \tag{10}$$

$$COV(z_1, z_2) = \frac{C}{2r_1 s_2}\sum_{p=1}^{r_1}\sum_{q=1}^{s_2}var\left(ln\frac{x_{i_p^1}}{x_{j_q^2}}\right) + \frac{C}{2r_2 s_1}\sum_{p=1}^{r_2}\sum_{q=1}^{s_1}var\left(ln\frac{x_{i_p^2}}{x_{j_q^1}}\right) - \frac{C}{2r_1 r_2}\sum_{p=1}^{r_1}\sum_{q=1}^{r_2}var\left(ln\frac{x_{i_p^1}}{x_{i_q^2}}\right) -$$

$$\frac{C}{2s_1 s_2}\sum_{p=1}^{s_1}\sum_{q=1}^{s_2}var\left(ln\frac{x_{j_p^1}}{x_{j_q^2}}\right), \tag{11}$$

$$CC = \frac{COV(z_1, z_2)}{\sqrt{var(z_1) \cdot var(z_2)}} \tag{12}$$

For soil PSF data, Eqs. (10~~), (11), and)~~ (12) can be simplified to three dimensions. The relationship between the ratios of soil PSF components and the dominant roles of ILR transformed data were indicated from the covariance structure. All ~~the~~ statistical analyses, such as the descriptive statistics of soil PSF data, calculation and evaluation of indicators, and the spatial prediction mapping, were performed using the R statistical program (R Development Core Team, 2019).

3 Results

3.1 Exploratory data analysis

3.1.1 Descriptive statistics of soil PSF data

From the descriptive statistics of the original (raw) and ILR transformed data, the silt fraction dominated the soil PSFs, ~~accounting for a more substantial amount~~larger than the sand and clay fractions. The distributions of the sand and clay fractions were similar (Fig. 2a). The ILR transformed data based on the three SBPs revealed different distributions (Figs. 2b~~, 2c, and~~

9

247   2d). For example, two ILR components (ILR1 and ILR2) for SBP1 had a symmetric distribution around zero ~~at~~on the *x*-axis

248   (Fig. 2b). In comparison, the distribution of data generated from SBP2 ~~or~~and SBP3 had a mirrored symmetry, with a left-

249   skewed ILR1 of SBP2 and right-skewed ILR2 of SBP3 (Figs. 2c and 2d). ~~The~~A comparison of means and medians

250   demonstrated that the back-transformed means of three sets of ILR transformed data were the same, and the mean ILR of sand

251   was closer to the median of sand compared with the original soil PSF data. In contrast, ~~the~~ opposite patterns were apparent for

252   the silt and clay components (Fig. 2e).

Center	Sand	Silt	Clay	Sand_ILR	Silt_ILR	Clay_ILR
Mean	19.61	66.80	13.59	18.07	71.48	10.45
Median	17.03	67.44	14.53	—	—	—

253
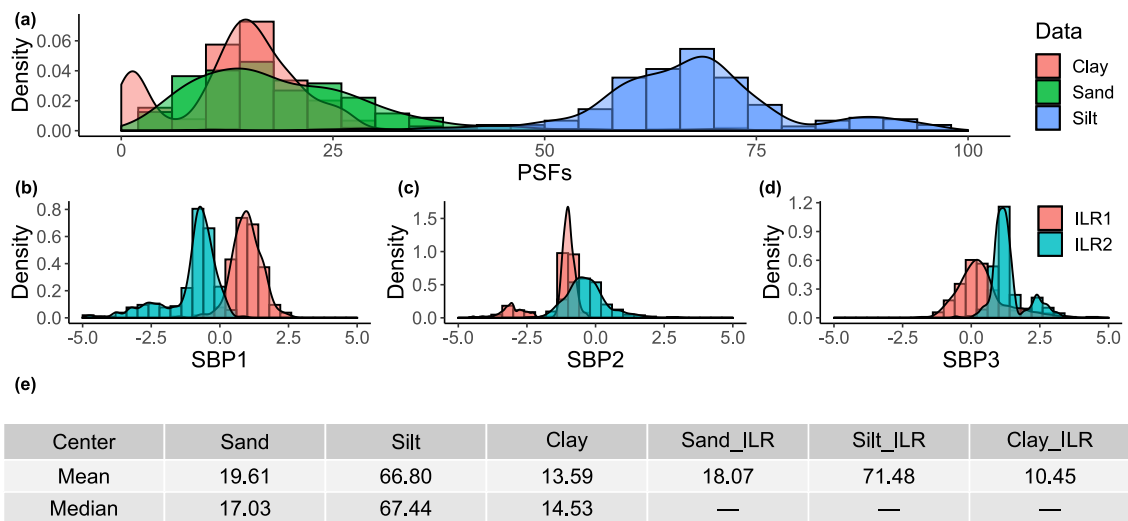
254 **Figure 2.** Descriptive statistics of original soil PSF and ILR transformed data using different SBPs. Note that the means of

255 Sand_ILR, Silt_ILR, and Clay_ILR from different SBPs were back-transformed ~~to the~~into real space.

256

257 **3.1.2 Covariance structure of ILR transformed data with different balances**

258   ~~The covariance~~Covariance analysis of the transformed data of soil PSFs based on the different SBPs showed that the

259 variance VarILR_1 of SBP3 was the largest, followed by ~~the~~that of VarILR_1 of SBP1 and SBP2 (Table 3). The variance of

260 the second component of ILR (VarILR_2) ~~followed the~~is opposite ~~pattern~~to that of VarILR_1. The COV and corresponding

261 CC followed the same ~~pattern~~law of SBP1 > SBP3 > SBP2. The first ILR equation (z_1 in Table 1) contained all the information

262 of soil PSFs, while the second ~~one~~ILR equation (z_2 in Table 1) included only two components. The information of VarILR_1

263 was therefore more abundant. All ~~of~~ VarILR_1 and VarILR_2 values were not 0 (or not nearly 0), indicating that there was no

264 constant (or almost constant) value in any two ratios of soil PSF components. The COV of SBP3 was close to 0, indicating

265 that the proportions of *clay/sand* and *clay/silt* were approximately the same. The same results were generated from the

266 corresponding CC. For the distribution of soil PSFs in a ternary diagram (the United States Department of Agriculture texture

267 triangle, USDA), the main texture class was silt loam (Fig. 3a). ~~The~~A biplot of soil samples demonstrated that the rays of the

10

268 three components, i.e., sand, silt, and clay, were reasonably well clustered at about 120° in the three groups (Fig. 3b).

269

270 **Table 3.** Covariance structure of soil PSFs based on different SBPs. VarILR_1 and VarILR_2 denote the variance of the first
271 and the second ~~component~~components of ILR, respectively. COV refers to the covariance of ILR1 and ILR2. CC is the
272 correlation coefficient.

Balances	VarILR_1	VarILR_2	COV	CC
SBP1	0.53	0.71	0.32	0.52
SBP2	0.39	0.86	-0.24	-0.41
SBP3	0.94	0.30	-0.09	-0.16

273

274
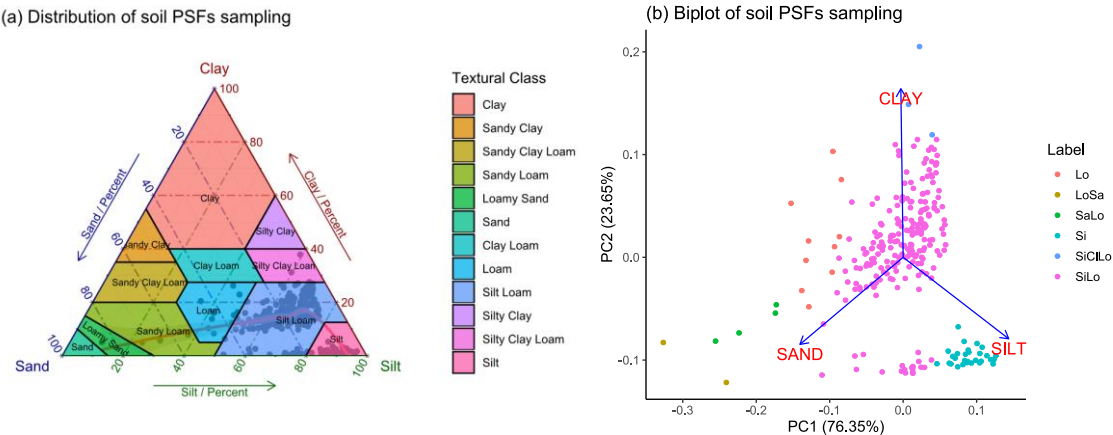
275 **Figure 3.** ~~The distribution~~Distribution of soil PSFs in the USDA triangle (a) and biplot graph (b). The red curve was fitted
276 ~~by~~using a loess function.

277 **3.2 ~~Accuracy comparison~~Comparison of the accuracy of different models using ILR data**

278 ~~The first three rows of the boxplots in Figs. 4a, 4b, and~~ To assess the accuracy of the different models, the Diebold–Mariano
279 test was used, which showed that the statistical differences of most models were significant. This significance was reflected
280 not only in different models (GLM and RF), but also in different SBPs when using the same model (Tables S6.1–S6.7). The
281 first three rows of the boxplots in Figs. 4a– 4c indicate the bias of the different models according to their ME values. The ME
282 of sand was closest to 0, followed by the MEs of clay and silt. GLM was more unbiased than RF, with lower ME values. After
283 combining with RK, there was ~~an~~a marked improvement in the ME for most GLM and RF models (Figs. 4a~~, 4b, and~~ 4c).
284 ~~For~~With respect to the accuracy assessment, the RMSE of silt was higher than ~~for~~that of the other two components. The
285 GLMRK did not perform as well as expected in terms of the RMSE, with only the sand component having an improved RMSE

11

286 (Fig. 4d). However, the RFRK performed better than the GLMRK and improved the accuracy of most ~~parts~~components
287 compared with the RF, except for the RFRK_SBP1 of sand. As an overall indicator, AD showed that the RF (or RFRK)
288 performed better than the GLM (or GLMRK) in terms of both average RMSE values and uncertainties (Fig. 4g). Moreover,
289 the RFRK improved the AD values for the SBP2 and SBP3 methods. ~~For~~With respect to the uncertainty assessment, the RF
290 generated lower uncertainties than the GLM according to bias, and the models combined with RK further reduced the
291 uncertainties, especially for the sand fractions of most ~~GLM and RF~~ models. (Table. S7.1).

292
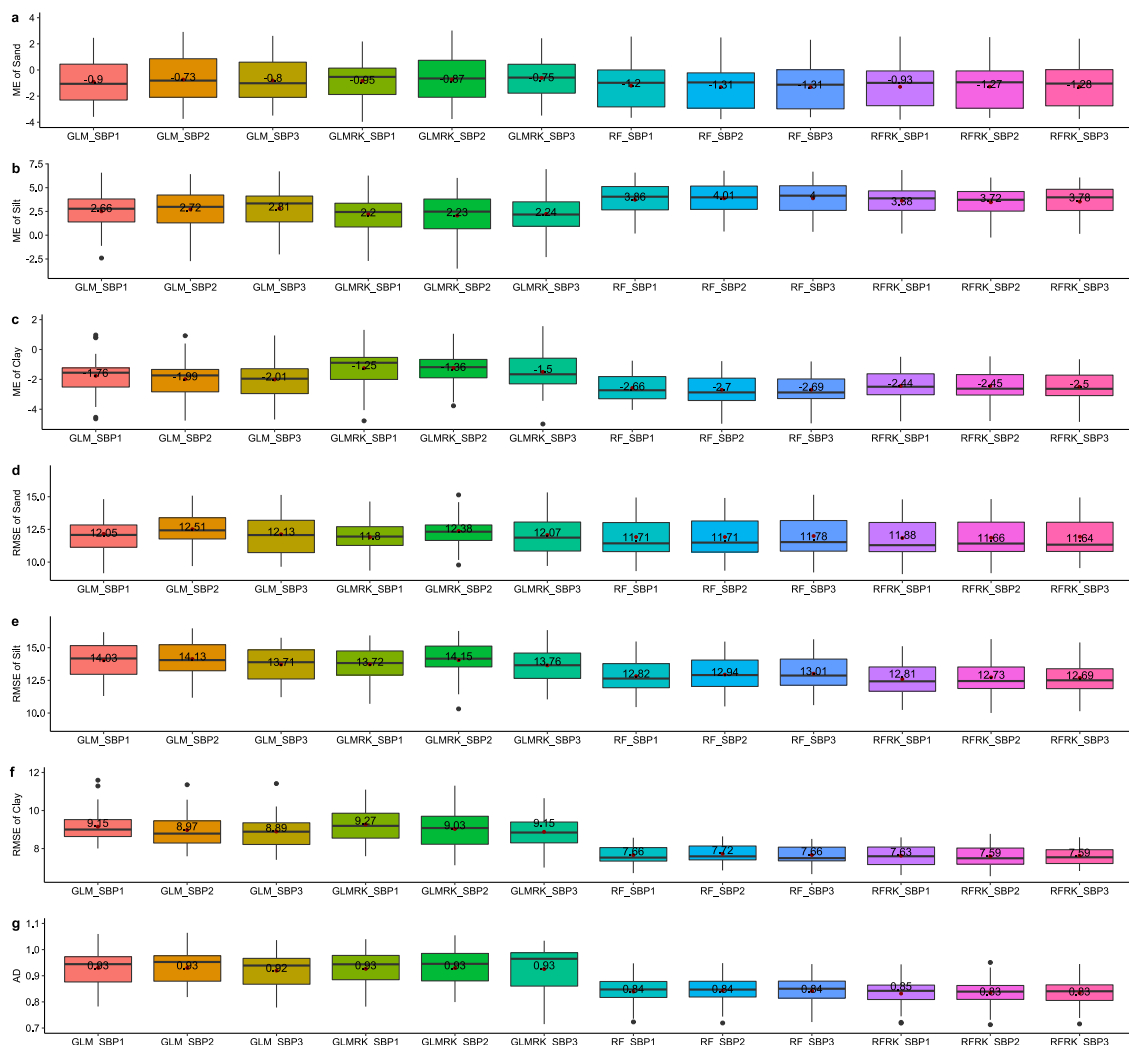
293 **Figure 4.** ~~Accuracy comparison~~Comparison of the accuracies of GLM, RF, and their RK patterns combined with three ILR
294 balances. The mean values of different model indicators were calculated in their boxes.

295

The model performances were different for the three SBPs. To better evaluate model performance using the different SBP balances, we graded each box from 1 to 3~~,~~ <u>based on the predicted results</u> and <u>Diebold–Mariano test results—</u>the final results are shown in Fig. 5. ~~The results demonstrated that~~ SBP1 performed best <u>in terms of bias</u>, with the lowest ME ~~value~~<u>score</u> of all models~~. For the~~<u>, except for GLMRK (Fig. 5a). With respect to the model</u> accuracy ~~comparison~~<u>assessment</u>, there was no apparent pattern, but <u>the</u> accuracy could be considered hierarchically: (1) for the GLM, ~~SBP1~~<u>SBP3</u> performed better than the other two SBP methods, ~~which also~~<u>and SBP1</u> performed well when ~~RK was~~ combined <u>with RK</u> (GLMRK); (2) for RF, SBP1 produced the best result. However, the introduction of RK resulted in the ~~Score2 of~~<u>SBP2 and</u> SBP3 performing ~~best among~~ ~~the three SBPs. However, RFRK of~~ <u>well (Fig. 5b). In addition, SBP3 and</u> SBP1 ~~performed worst according to the values of~~ ~~Score2 and Score5.~~<u>delivered a better performance for GLM and RF, respectively (Figs. 5c–5e).</u> Finally, ~~for the~~<u>in a</u> comprehensive assessment, SBP1 performed best ~~among~~<u>out of the</u> three SBPs according to ~~Score6.~~<u>SUM6 (Fig. 5f).</u> More details and ~~calculation processes~~<u>calculations</u> can be found in the Supplementary Material (Table S4.1).

13
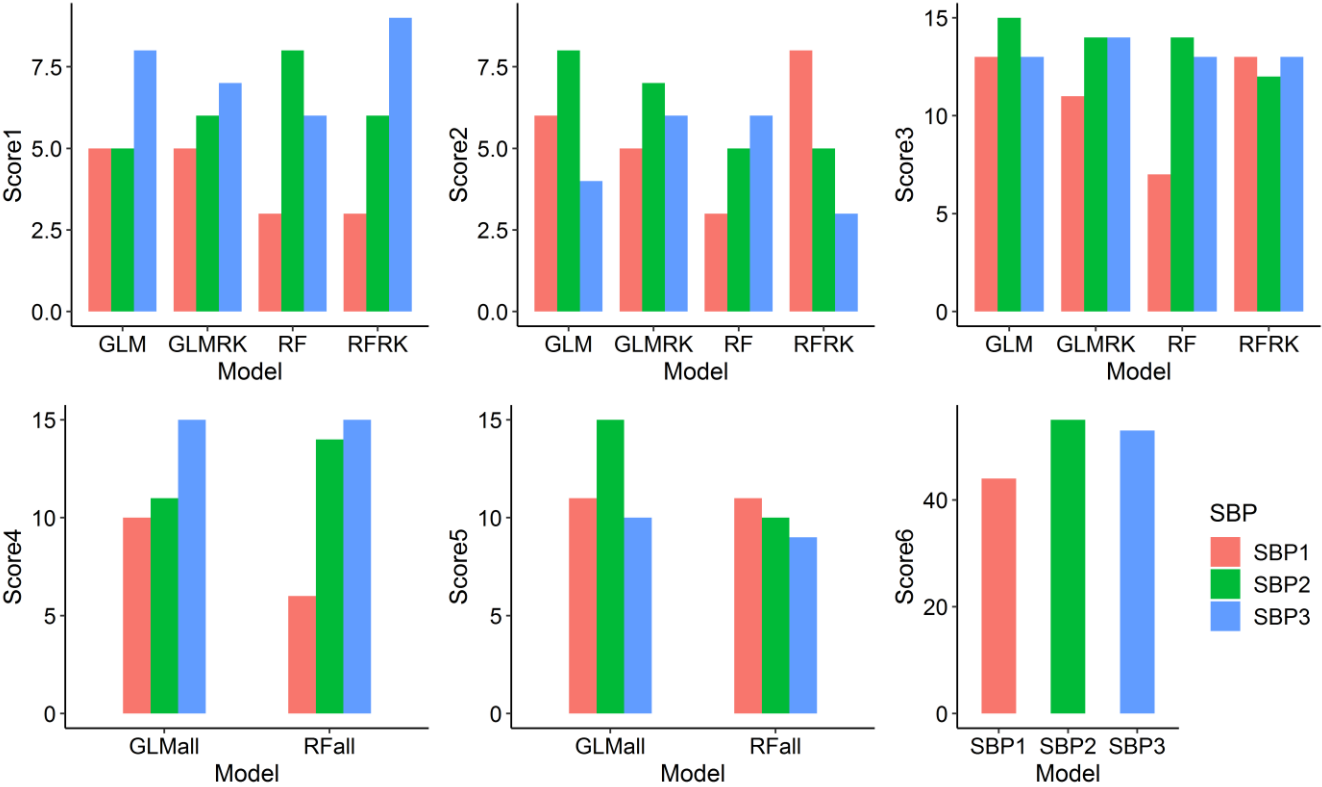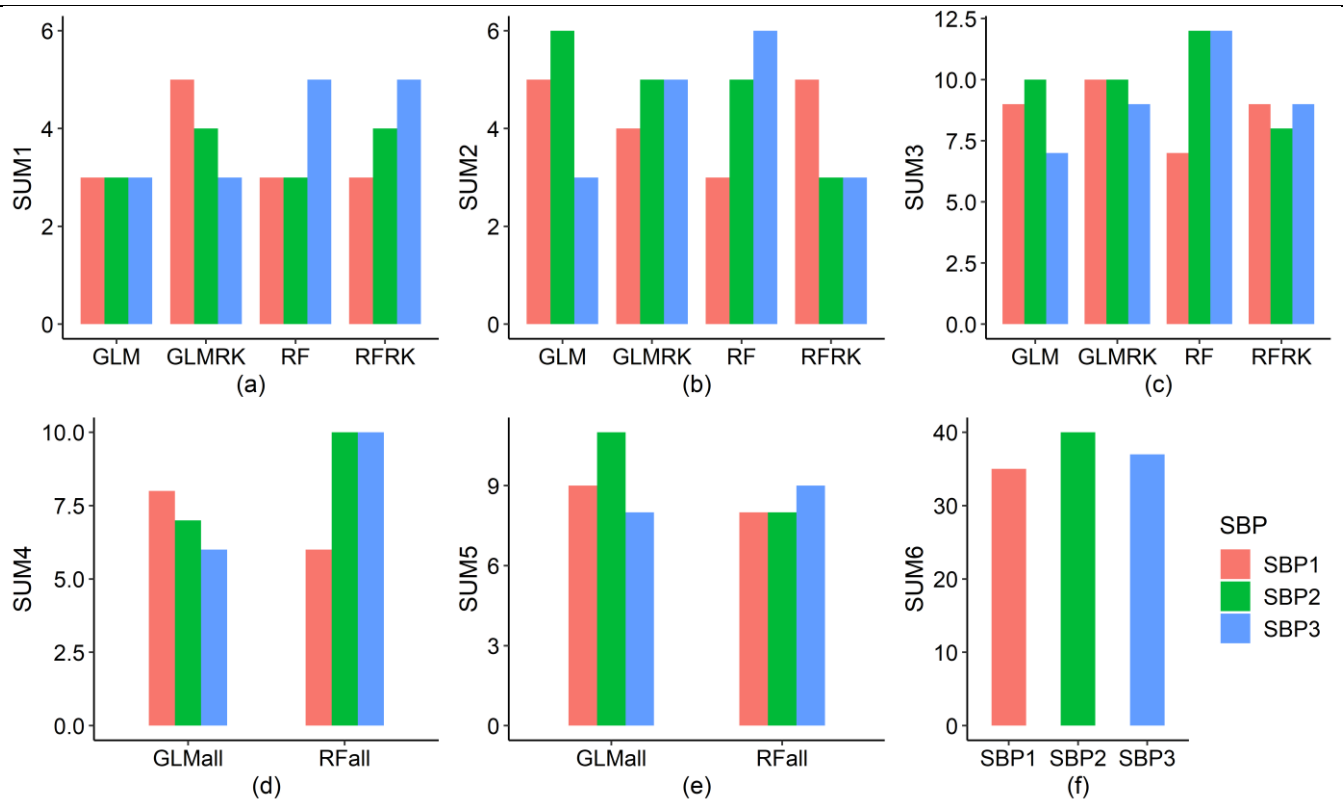
Figure 5. Ranking score of model performance based on three SBPs. ~~Score1~~SUM1 (a) and ~~Score2~~SUM2 (b) are the sum scores of ME and RMSE for each model, respectively~~; Score3~~. SUM3 (c) is the sum ~~scores~~score of ME, RMSE, and AD for each model~~, Score4~~; SUM4 (d) and ~~Score5~~SUM5 (e) are the sum scores of ME or RMSE for GLM_all (GLM and GLMRK) and RF_all (RF and RFRK~~), Score6~~); SUM6 (f) is the sum ~~scores~~score of all indicators. The lower the value of these scores, the better the model performance.

3.3 Spatial prediction maps of soil PSFs generated from the different models

Prediction maps of soil PSFs ~~made~~constructed from the different models are shown in Figs. 6, S3.1, and S3.2. For the components of soil PSFs, the prediction maps of the three ~~group maps~~components followed a similar rule. The GLM and GLMRK produced ~~more extensive~~broader ranges of predicted values, and their maps were more relevant to the real environment. However, the RF and RFRK predicted a relatively narrow range of low values for these components~~,~~ (sand, silt and clay), revealing a smoother distribution than that generated by the GLM and GLMRK. Unlike the regression methods, the ~~RF~~hybrid methods (GLMRK and RFRK ~~methods~~) produced hot and cold spots on the prediction maps and more details of the soil sampling points were apparent (Fig. S5.1).

14

(a) GLM_SBP1 **(b) GLM_SBP2** **(c) GLM_SBP3**

(d) GLMRK_SBP1 **(e) GLMRK_SBP2** **(f) GLMRK_SBP3**

(g) RF_SBP1 **(h) RF_SBP2** **(i) RF_SBP3**

(j) RFRK_SBP1 **(k) RFRK_SBP2** **(l) RFRK_SBP3**

Sand (%)

| 0 - 11 | 16 - 20 | 24 - 29 | 36 - 50 |
| 11 - 16 | 20 - 24 | 29 - 36 | 50 - 75 |

0 40 80 160 240 320 km
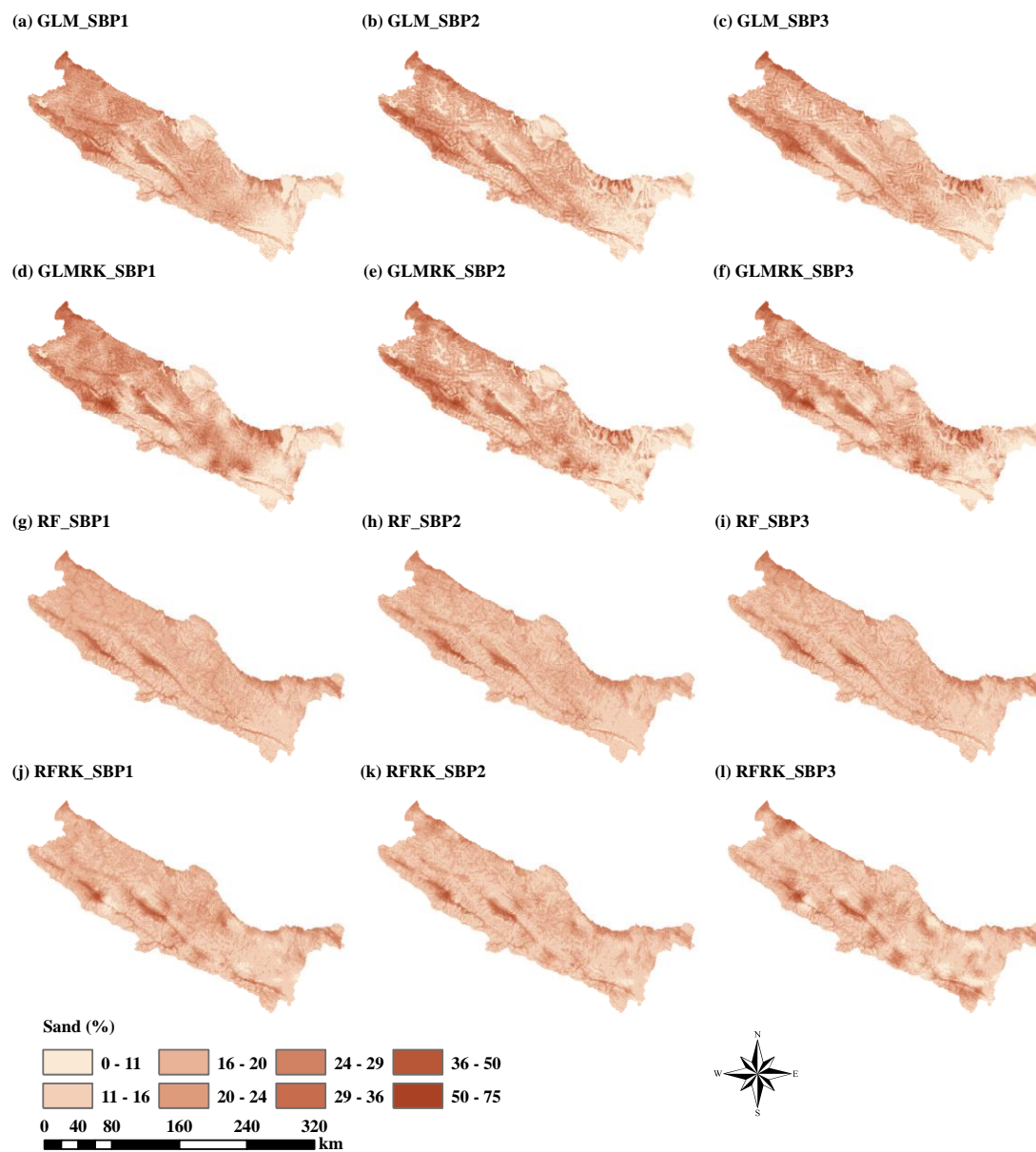
Figure 6. Spatial prediction maps of the sand component of the upper reaches of the Heihe River Basin.

3.4 Spatial distribution of soil texture classes in the USDA triangles

The predicted soil textures in the USDA texture triangles (Fig. 7) showed that most predictions fell within the range of observed soil textures (Fig. 3a), and silt loam was the dominant soil texture in all cases. The GLM produced a more discrete distribution than the RF, and the RK method expanded the dispersion. ~~In the~~With respect to trends ~~of~~in the predicted samples, the silt

15

329 components predicted from all models were overestimated. The pattern fitting curves indicated that the prediction results were

330 closer to the bottom right of the USDA triangle than the soil PSF observations. The GLMRK and RFRK curves were longer

331 than the GLM and RF curves, with a more extensive range of values in triangles. Compared with the GLMRK, the RFRK

332 produced a more upward extension (Figs. 7j, k, l 7l). It was clear that the clay fraction was overestimated and the sand fraction

333 was underestimated.
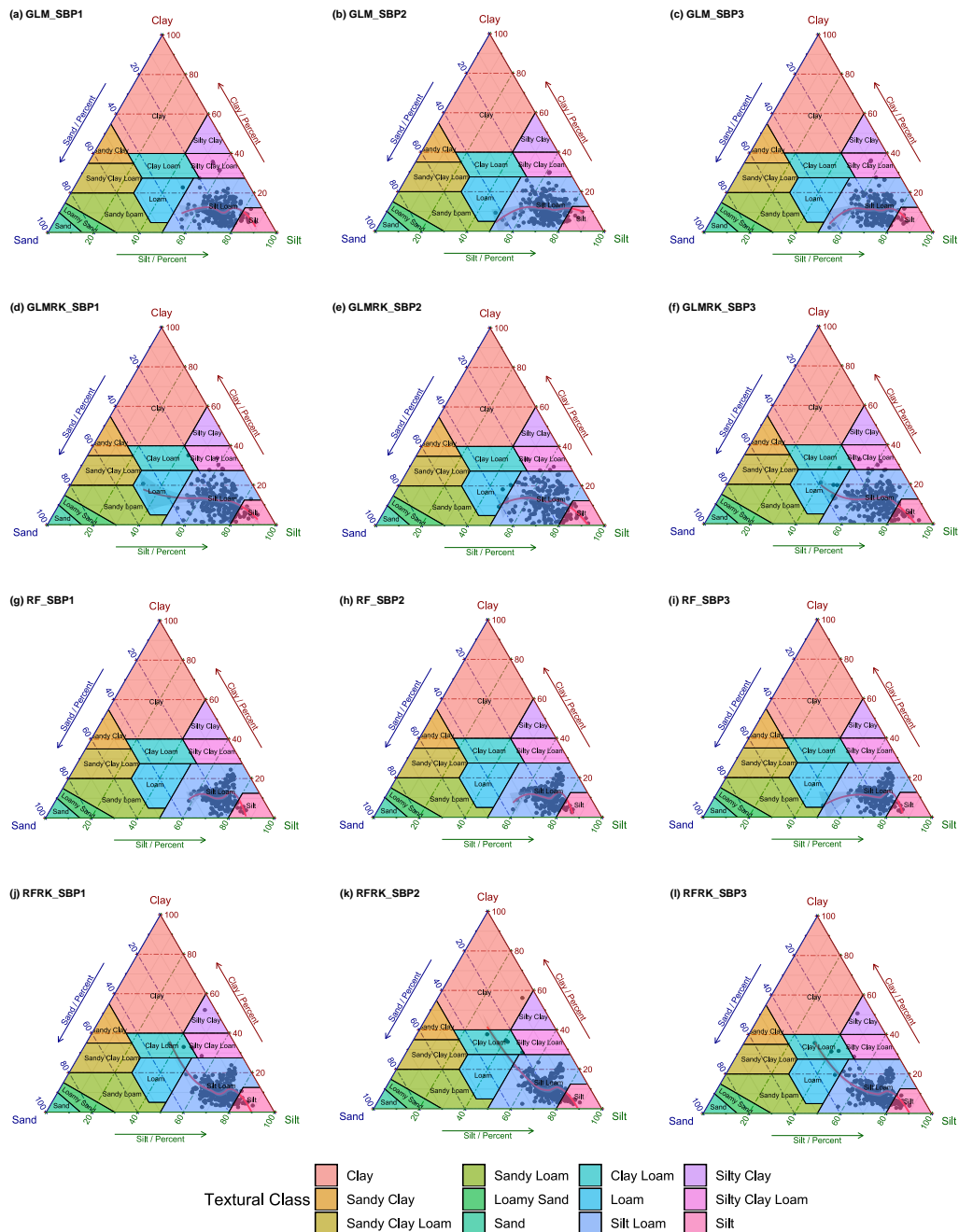
Figure 7. Predicted 262 soil samples in USDA texture triangles using (a) GLM_SBP1, (b) GLM_SBP2, (c) GLM_SBP3, (d) GLMRK_SBP1, (e) GLMRK_SBP2, (f) GLMRK_SBP3, (g) RF_SBP1, (h) RF_SBP2, (i) RF_SBP3, (j) RFRK_SBP1, (k)

17

337 RFRK_SBP2, ~~and~~ (l) RFRK_SBP3. Red fitting curves ~~in triangles showed~~show the trends.

4 Discussion

4.1 Comparison of the GLM, RF, and RK patterns using ILR data

340 We found that RF ~~reveal~~provided more accurate results, but with more bias than the GLM, and that the RK method improved
341 the performance in terms of bias for most models and ~~the~~accuracy of the RF. Odeh et al. (1995) indicated that RK was superior
342 to ~~the~~ linear models, such as MLR, which was reflected in the prediction results for sand in our study. Scarpone et al. (2016)
343 reported that as a hybrid interpolator, the RFRK outperformed the RF when making soil thickness predictions. We proved that
344 RFRK was also suitable for compositional data and improved model performance when ~~combining~~combined with the ILR
345 transformation. In summary, the GLM and RF had both advantages and disadvantages when considering the trade-off between
346 bias and accuracy.

347 The results of GLM and GLMRK should not depend on the choice of ILR basis ~~being chosen~~, which has been proved by
348 previous studies on the use of linear models and kriging for compositional data (Pawlowsky-Glahn et al, 2015). However, the
349 GLM model used the "glmStepAIC" algorithm (i.e., a stepwise regression) to select the best combination of environmental
350 covariables for each ILR component (Table S2.1). Therefore, the variable inputs are different for these ILR data, and further
351 impact the accuracy assessment and prediction maps. In addition, the difficulty with ~~the use of the~~ GLM is the need for a back-
352 transformation. There is a need to present results on the original untransformed scale after conducting the analysis on a
353 transformed level, which may produce spurious results (Lane, 2002). In our study, we compared the means of ILR transformed
354 data and the original data. We proved the feasibility of the ILR transformation method, especially for meeting the requirements
355 of compositional data. However, the accuracy of the GLM still needs to be improved, which may be because the transformed
356 data did not follow a normal distribution (Fig. 2). With respect to uncertainty, the uncertainty of bias for GLM is higher than
357 that of RF, but the uncertainty of accuracy for GLM is lower. However, RF performed better in terms of accuracy assessment.
358 Therefore, the main concern was whether the introductions of RK could reduce the uncertainty of RF. With regard to the
359 performances of RFRK and RF, adding RK was recommended in soil PSF interpolation combined with ILR transformed data.
360 In addition, the range of 95% prediction interval for different models (Figs. S8.1–8.6) demonstrated that the differences were
361 very close. This may because the values of variance for ILR data were small, showing low uncertainty when using ILR
362 transformed data.

363 Although the RF had the advantage of prediction accuracy, the limited interpretability of the consequences made it difficult
364 to modify the prediction bias—each tree from the model ~~cannot~~could not be examined individually (Grimm et al., 2008).
365 Moreover, the ILR transformation before modeling increased the difficulty of interpretation for not only the predicted values
366 on the ILR scale but also the residuals. The back-transformation of the optimal estimate of log-ratio variables ~~does~~did not
367 generate ~~the~~an optimal estimation of compositional data (Lark and Bishop, 2007), which should also be considered.

4.2 Comparison of three SBPs of ILR transformation

~~For the comparison of~~Regarding the three SBPs, the ME and RMSE performed better when using SBP1 for ILR transformed data, which may be interpreted as the distributions of the ILR1 and ILR2 of SBP1 being more symmetric (Fig. 2b). In contrast, the performance of SBP2 was worse than that of SBP1 and SBP3 because the ILR_1 component, including all the soil PSF information, was left-skewed (Fig. 2c). This result was especially apparent for the GLM and GLMRK, because the data in a linear model needs to be normally distributed (Lane, 2002).

The negligible difference among the three SBP balances revealed a triangular shape with a cluster at about 120° (Fig. 3b). This could be interpreted as the three soil PSFs having a mixed pattern, with each component dominated by the components in one cluster (Tolosana-Delgado et al., 2005). Although the silt component dominated the soil PSFs (Fig. 2a), sand and clay also played important roles in soil ~~compositions~~composition. Taking either the most abundant component of the compositional data as the denominator (Martins et al., 2016) or the first component of the permutations did not provide convincing evidence~~.~~ ~~Because~~ that the model performs best. This is because using the most abundant component of the compositional data as the primary component of the alterations, i.e., SBP2, resulted in a relatively poor performance compared to the other SBPs. Thus, we recommend that the focus should be on data distribution. Furthermore, the choice of balance and combination of RK are also the key to improving model accuracy, as shown by the result of the RFRK-SBP3 model (Fig. 4).

4.3 Limitations

Firstly, the scope of this study is limited to independent modeling. Each ILR component was modeled separately, which may be suboptimal because ~~they~~the components cannot ~~further consider~~take into account the cross correlations among the ILR coordinates. However, the study has demonstrated the relation of the raw data (sand, silt, and clay~~),~~) based on ILR transformation, and has confirmed that ~~the~~ currently used prediction models in this work are suitable. In our pervious study, we have used compositional kriging (CK) for the spatial prediction of soil PSFs (Wang and Shi, 2017), and the cross correlations of ILRs can be taken into account using CK. Although ~~it~~CK is optimal, it cannot ~~consider~~take into account different balances of ILR, nor can it be combined with ~~the~~a hybrid interpolator (e.g., RK). Moreover, predicting each ILR component separately was a more suitable approach for the spatial prediction models currently used (such as the GLM and RF). Therefore, more alternative spatial prediction models combined with interpretation of ILR balances for compositional data should be considered in the future. For example, CK and high-accuracy surface modelling (HASM; Yue et al., 2007; Yue, 2011; Yue et al., 2016) can be applied for small scale study areas. For large scale study areas, multivariate RF (Segal and Xiao, 2011) can be combined with a log-ratio transformation and hybrid interpolation ~~method~~methods, enabling the cross correlations among ILR coordinates to be better interpreted.

Secondly, the weighting problem was not considered in this study~~,~~ because the ILR method can be qualified as an unweighted log-ratio transformation, giving all parts the same weight for both the definition of the total variance and the reduction of

dimension~~dimensions~~. This may enlarge the ratios generated from the rare ~~parts~~component, which would dominate the analysis (Greenacre and Lewi, 2009). The pairwise log-ratio can be used to set weights by their proportions when there is no ~~additional~~ knowledge ~~about~~of the component measurement errors (Greenacre, 2019). Nevertheless, all three parts of the soil PSF data dominated the biplot diagram, without the influence of rare elements and with no redundancy; thus, none of the shortcomings mentioned above were apparent. Accuracy assessments using a pairwise log-ratio transformation require further study in the future.

5 Conclusions

We evaluated and compared the ~~performance~~performances of the GLM~~,~~ and the RF~~,~~ and their hybrid ~~pattern~~patterns (i.e., GLMRK and RFRK) using different balances of ILR transformed data. The bias of the GLM was lower than that of the RF; however, the accuracy of the GLM was relatively low. More discrete distributions and broader ranges of prediction value distributions were produced from GLMs in the USDA soil texture triangles. In other words, different predicted data sets were generated from the use of the GLM and RF, with unbiased and inaccurate predictions for the GLM and biased and more accurate predictions for the RF.

The hybrid patterns, GLMRK and RFRK, were found to ~~be~~provide the best ~~solution~~solutions because ~~it~~they produced a relatively high prediction accuracy and strong correlations with ECs, providing more details about the soil sampling points (hot spots and cold spots) compared with ~~only~~using the regression model only. However, the non-normal distribution of ILR data and ~~its~~their residuals, and ~~more~~increased data transformation and inverse transformation ~~processes~~, make models ~~further~~more difficult to ~~interpreted~~interpret and improve.

~~For the different SBPs, the~~The three SBP-based ~~data~~datasets generated different distributions~~, but~~; a statistical significance test proved that most models had significant differences in prediction accuracy using different SBPs. A ranking score was provided to demonstrate these differences, and compositional balance should be considered when mapping soil PSFs. However, no pattern was apparent~~. This~~, which could be explained by the angle of the biplot diagram~~, ~~with three rays of soil PSF components clustered into three modes, and each part dominating its cluster. Using the most abundant component of the compositional data as the first component of the permutations was not considered the ~~right~~best choice for mapping soil PSFs because SBP2 ~~produced~~delivered the worst performance. Thus, we recommend that the focus should be on data distribution. This study ~~can provide~~provides a reference for the spatial simulation of soil PSFs combined with ECs at the regional scale, and ~~how to choose~~for choosing the balances of ILR transformed data.

Data Availability. We did not use any new data and the data we used come from previously published sources. Soil particle-size fractions data is available through our previous studies (Wang and Shi, 2017, 2018). Moreover, it also can be visited on this website: http://data.tpdc.ac.cn/zh-hans/data/7f91d36d-8bbd-40d5-8eaf-7c035e742f40/ (Digital soil mapping dataset of soil texture (soil particle-size fractions) in the upstream of the Heihe river basin (2012-2016); last access: 4 July 2020). The

meteorological data can be accessed through http://data.cma.cn/ (last access: 4 July 2020). Environmental covariates data of soil physical and chemical properties and categorical maps can be obtained through http://data.tpdc.ac.cn/zh-hans/ (last access: 4 July 2020), including saturated water content, field water holding capacity, wilt water content, saturated hydraulic conductivity data (http://data.tpdc.ac.cn/zh-hans/data/e977f5e8-972b-42a5-bffe-cd0195f3b42b/, Digital soil mapping dataset of hydrological parameters in the Heihe River Basin (2012); last access: 4 July 2020), and soil thickness data (http://data.tpdc.ac.cn/zh-hans/data/fc84083e-8c66-4a42-b729-4f19334d0d67/, Digital soil mapping dataset of soil depth in the Heihe River Basin (2012-2014); last access: 4 July 2020). DEM data set is provided by the Geospatial Data Cloud site, Computer Network Information Center, Chinese Academy of Sciences. (http://www.gscloud.cn, last access: 4 July 2020).

Author contribution. Wenjiao Shi contributed to soil data sampling, oversaw the design of the entire project. Mo Zhang performed the model analysis and wrote the manuscript. Both authors contributed to writing this paper and interpreting data.

Competing interests. The authors declare that they have no conflict of interest.

References

Aitchison, J.: The statistical analysis of compositional data, Chapman and Hall, Ltd., 416 pp., 1986.

Akpa, S. I. C., Odeh, I. O. A., Bishop, T. F. A., and Hartemink, A. E.: Digital mapping of soil particle-size fractions for Nigeria, Soil Sci. Soc. Am. J., 78, 1953-1966, https://doi.org/10.2136/sssaj2014.05.0202, 2014.

Bishop, T. F. A., and McBratney, A. B.: A comparison of prediction methods for the creation of field-extent soil property maps, Geoderma, 103, 149-160, https://doi.org/10.1016/S0016-7061(01)00074-X, 2001.

Breiman, L.: Bagging predictors, Machine Learning, 24, 123-140, https://doi.org/10.1023/a:1018054314350, 1996.

Breiman, L.: Random forests, Machine Learning, 45, 5-32, https://doi.org/10.1023/a:1010933404324, 2001.

Buchanan, S., Triantafilis, J., Odeh, I. O. A., and Subansinghe, R.: Digital soil mapping of compositional particle-size fractions using proximal and remotely sensed ancillary data, Geophysics, 77, WB201-WB211, https://doi.org/10.1190/geo2012-0053.1, 2012.

Coenders, G., Martin-Fernandez, J.A., Ferrer-Rosell, B.: When relative and absolute information matter: Compositional predictor with a total in generalized linear models. Statistical Modelling 17(6), 494-512, 2017.

Conrad, O., Bechtel, B., Bock, M., Dietrich, H., Fischer, E., Gerlitz, L., Wehberg, J., Wichmann, V., and Böhner, J.: System for automated geoscientific analyses (SAGA) v. 2.1.4, Geosci. Model Dev., 8, 1991-2007, https://doi.org/10.5194/gmd-8-1991-2015, 2015.

Delbari, M., Afrasiab, P., and Loiskandl, W.: Geostatistical analysis of soil texture fractions on the field scale, Soil and Water Research, 6, 173-189, https://doi.org/10.17221/9/2010-SWR, 2011.

Diebold, F.X. and Mariano, R.S.: Comparing predictive accuracy. Journal of Business and Economic Statistics, 13, 253-263, 1995.

Egozcue, J. J., Pawlowsky-Glahn, V., Mateu-Figueras, G., and Barcelo-Vidal, C.: Isometric logratio transformations for compositional data analysis, Mathematical Geology, 35, 279-300, https://doi.org/10.1023/a:1023818214614, 2003.

Egozcue, J. J., and Pawlowsky-Glahn, V.: Groups of parts and their balances in compositional data analysis, Mathematical Geology, 37, 795-828, https://doi.org/10.1007/s11004-005-7381-9, 2005.

Facevicova, K., Hron, K., Todorov, V., and Templ, M.: General approach to coordinate representation of compositional tables. Scandinavian Journal of Statistics 45(4), 879-899, 2018.

Filzmoser, P., and Hron, K.: Correlation analysis for compositional data, Math Geosci., 41, 905-919, https://doi.org/10.1007/s11004-008-9196-y, 2009.

Filzmoser, P., Hron, K., and Reimann, C.: Univariate statistical analysis of environmental (compositional) data: Problems and possibilities, Sci. Total Environ., 407, 6100-6108, https://doi.org/10.1016/j.scitotenv.2009.08.008, 2009.

Fiserova, E., and Hron, K.: On the interpretation of orthonormal coordinates for compositional data, Math Geosci., 43, 455-468, https://doi.org/10.1007/s11004-011-9333-x, 2011.

Goovaerts, P.: Geostatistics in soil science: state-of-the-art and perspectives, Geoderma, 89, 1-45, https://doi.org/10.1016/S0016-7061(98)00078-0, 1999.

Greenacre, M., and Lewi, P.: Distributional equivalence and subcompositional coherence in the analysis of compositional data, contingency tables and ratio-scale measurements, Journal of Classification, 26, 29-54, https://doi.org/10.1007/s00357-009-9027-y, 2009.

Greenacre, M.: variable selection in compositional data analysis using pairwise logratios, Math Geosci., 51, 649-682, https://doi.org/10.1007/s11004-018-9754-x, 2019.

Grimm, R., Behrens, T., Märker, M., and Elsenbeer, H.: Soil organic carbon concentrations and stocks on Barro Colorado

Island – Digital soil mapping using Random Forests analysis, Geoderma, 146, 102-113, https://doi.org/10.1016/j.geoderma.2008.05.008, 2008.

Harvey, D., Leybourne, S., and Newbold, P.: Testing the equality of prediction mean squared errors. International Journal of forecasting, 13(2), 281-291, 1997.

Hengl, T., Heuvelink, G. B. M., and Stein, A.: A generic framework for spatial prediction of soil variables based on regression-kriging, Geoderma, 120, 75-93, https://doi.org/10.1016/j.geoderma.2003.08.018, 2004.

Hengl, T., Heuvelink, G. B. M., Kempen, B., Leenaars, J. G. B., Walsh, M. G., Shepherd, K. D., Sila, A., MacMillan, R. A., de Jesus, J. M., Tamene, L., and Tondoh, J. E.: Mapping soil properties of Africa at 250 m resolution: random forests significantly improve current predictions, Plos One, 10, 26, https://doi.org/10.1371/journal.pone.0125814, 2015.

Hengl, T., Mendes de Jesus, J., Heuvelink, G. B. M., Ruiperez Gonzalez, M., Kilibarda, M., Blagotić, A., Shangguan, W., Wright, M. N., Geng, X., Bauer-Marschallinger, B., Guevara, M. A., Vargas, R., MacMillan, R. A., Batjes, N. H., Leenaars, J. G. B., Ribeiro, E., Wheeler, I., Mantel, S., and Kempen, B.: SoilGrids250m: Global gridded soil information based on machine learning, Plos One, 12, e0169748, https://doi.org/10.1371/journal.pone.0169748, 2017.

Hiemstra, P. H., Pebesma, E. J., Twenhöfel, C. J. W., and Heuvelink, G. B. M.: Real-time automatic interpolation of ambient gamma dose rates from the Dutch radioactivity monitoring network, Computers & Geosciences, 35, 1711-1721, https://doi.org/10.1016/j.cageo.2008.10.011, 2009.

Keskin, H., and Grunwald, S.: Regression kriging as a workhorse in the digital soil mapper's mapper's toolbox, Geoderma, 326, 22-41, https://doi.org/10.1016/j.geoderma.2018.04.004, 2018.

K. Gerald van den Boogaart, and Raimon Tolosana, M. B Matevz Bren.: Compositions: compositional data analysis, R package version 1.40-1 ed., available at: https://cran.rstudio.com/web/packages/compositions/index.html (last access: 14 July 2020), 2014.

Lane, P. W.: Generalized linear models in soil science, European Journal of Soil Science, 53, 241-251, https://doi.org/10.1046/j.1365-2389.2002.00440.x, 2002.

Lark, R. M.: A comparison of some robust estimators of the variogram for use in soil survey, European Journal of Soil Science, 51, 137-157, https://doi.org/10.1046/j.1365-2389.2000.00280.x, 2000.

Lark, R. M.: Two robust estimators of the cross-variogram for multivariate geostatistical analysis of soil properties, European Journal of Soil Science, 54, 187-201, https://doi.org/10.1046/j.1365-2389.2003.00506.x, 2003.

Lark, R. M., and Bishop, T. F. A.: Cokriging particle size fractions of the soil, Eur. J. Soil Sci., 58, 763-774, https://doi.org/10.1111/j.1365-2389.2006.00866.x, 2007.

Liaw, A., and Wiener, M.: Classification and regression by random forest, 23, available at: https://cran.r-project.org/web/packages/randomForest/index.html (last access: 14 July 2020), 2001.

Ließ, M., Glaser, B., and Huwe, B.: Uncertainty in the spatial prediction of soil texture: Comparison of regression tree and

Random Forest models, Geoderma, 170, 70–79, https://doi.org/10.1016/j.geoderma.2011.10.010, 2012.

Lloyd, C. D., Pawlowsky-Glahn, V., and Jose Egozcue, J.: Compositional data analysis in population studies, Annals of the Association of American Geographers, 102, 1251-1266, https://doi.org/10.1080/00045608.2011.652855, 2012.

Martins, A. B. T., Bonat, W. H., and Ribeiro, P. J.: Likelihood analysis for a class of spatial geostatistical compositional models, Spat. Stat., 17, 121-130, https://doi.org/10.1016/j.spasta.2016.06.008, 2016.

Max Kuhn: Caret: Classification and regression training, R package version 6.0-80 ed., available at: https://cran.r-project.org/web/packages/caret/index.html (last access: 14 July 2020), 2018.

McBratney, A. B., Minasny, B., Cattle, S. R., and Vervoort, R. W.: From pedotransfer functions to soil inference systems, Geoderma, 109, 41-73, https://doi.org/10.1016/S0016-7061(02)00139-8, 2002.

McBratney, A. B., Santos, M. L. M., and Minasny, B.: On digital soil mapping, Geoderma, 117, 3-52, https://doi.org/10.1016/s0016-7061(03)00223-4, 2003.

Menafoglio, A., Guadagnini, A., and Secchi, P.: A kriging approach based on Aitchison geometry for the characterization of particle-size curves in heterogeneous aquifers, Stochastic Environmental Research and Risk Assessment, 28, 1835-1851, https://doi.org/10.1007/s00477-014-0849-8, 2014.

Menafoglio, A., Guadagnini, A., and Secchi, P.: A kriging approach based on Aitchison geometry for the characterization of particle-size curves in heterogeneous aquifers, Stoch. Environ. Res. Risk Assess., 28, 1835-1851, https://doi.org/10.1007/s00477-014-0849-8, 2014.

Menafoglio, A., Secchi, P., and Guadagnini, A.: A class-kriging predictor for functional compositions with application to particle-size curves in heterogeneous aquifers, Math Geosci., 48, 463-485, https://doi.org/10.1007/s11004-015-9625-7, 2016a.

Menafoglio, A., Guadagnini, A., and Secchi, P.: Stochastic simulation of soil particle-size curves in heterogeneous aquifer systems through a Bayes space approach, Water Resources Research, 52, 5708-5726, https://doi.org/10.1002/2015wr018369, 2016b.

Molayemat, H., Torab, F. M., Pawlowsky-Glahn, V., Morshedy, A. H., and Jose Egozcue, J.: The impact of the compositional nature of data on coal reserve evaluation, a case study in Parvadeh IV coal deposit, Central Iran, International Journal of Coal Geology, 188, 94-111, https://doi.org/10.1016/j.coal.2018.02.003, 2018.

Nelder, J. A., and Wedderburn, R. W. M.: Generalized linear models, Journal of the Royal Statistical Society. Series A (General), 135, 370-384, https://doi.org/10.2307/2344614, 1972.

Nickel, S., Hertel, A., Pesch, R., Schroeder, W., Steinnes, E., and Uggerud, H. T.: Modelling and mapping spatio-temporal trends of heavy metal accumulation in moss and natural surface soil monitored 1990-2010 throughout Norway by multivariate generalized linear models and geostatistics, Atmospheric Environment, 99, 85-93, https://doi.org/10.1016/j.atmosenv.2014.09.059, 2014.

24

Odeh, I. O. A., McBratney, A. B., and Chittleborough, D. J.: Further results on prediction of soil properties from terrain attributes: heterotopic cokriging and regression-kriging, Geoderma, 67, 215-226, https://doi.org/10.1016/0016-7061(95)00007-B, 1995.

Pawlowsky-Glahn, V.: On spurious spatial covariance between variables of constant sum, 107-113 pp., 1984.

Pawlowsky-Glahn V, Egozcue JJ, Tolosana-Delgado R.: Modeling and analysis of compositional data. John Wiley & Sons, Ltd, 2015.

R Development Core Team: R: A language and environment for statistical computing, in, R Foundation for Statistical Computing, Vienna, Austria, 2019.

Scarpone, C., Schmidt, M. G., Bulmer, C. E., and Knudby, A.: Modelling soil thickness in the critical zone for Southern British Columbia, Geoderma, 282, 59-69, https://doi.org/10.1016/j.geoderma.2016.07.012, 2016.

Segal, M. and Xiao, Y. Y.: Multivariate random forests,Wiley Interdisciplinary Reviews-Data Mining and Knowledge Discovery, 1, 80–87, https://doi.org/10.1002/widm.12, 2011.

Shi, W.J., Liu, J.Y., Du, Z.P., Song, Y.J., Chen, C.F. and Yue, T.X.: Surface modelling of soil pH. Geoderma 150, 113-119, 2009

Shi, W.J., Liu, J.Y., Du, Z.P., Stein, A. and Yue, T.X.: Surface modeling of soil properties based on land use information. Geoderma 162, 347-357, 2011.

Shi W.J., Yue T.X., Du Z.P., Wang Z, Li X.W.: Surface Modeling of Soil antibiotics. Science of the Total Environment, 543(2): 609-619, 2016.

Song, X.-D., Brus, D. J., Liu, F., Li, D.-C., Zhao, Y.-G., Yang, J.-L., and Zhang, G.-L.: Mapping soil organic carbon content by geographically weighted regression: A case study in the Heihe River Basin, China, Geoderma, 261, 11-22, https://doi.org/10.1016/j.geoderma.2015.06.024, 2016.

Talska, R., Menafoglio, A., Machalova, J., Hron, K., and Fiserova, E.: Compositional regression with functional response, Computational Statistics & Data Analysis, 123, 66-85, 10.1016/j.csda.2018.01.018, 2018.

Tolosana-Delgado, R., Otero, N., Pawlowsky-Glahn, V., and Soler, A.: Latent compositional factors in the Llobregat River Basin (Spain) hydrogeochemistry, Mathematical Geology, 37, 681-702, https://doi.org/10.1007/s11004-005-7375-7, 2005.

Venables, W. N., and Dichmont, C. M.: GLMs, GAMs and GLMMs: an overview of theory for applications in fisheries research, Fisheries Research, 70, 319-337, https://doi.org/10.1016/j.fishres.2004.08.011, 2004.

Walvoort, D. J. J., and de Gruijter, J. J.: Compositional Kriging: A spatial interpolation method for compositional data, Mathematical Geology, 33, 951-966, https://doi.org/10.1023/a:1012250107121, 2001.

Wang, Z., and Shi, W. J.: Mapping soil particle-size fractions: A comparison of compositional kriging and log-ratio kriging, J. Hydrol., 546, 526-541, https://doi.org/10.1016/j.jhydrol.2017.01.029, 2017.

Wang, Z., and Shi, W. J.: Robust variogram estimation combined with isometric log-ratio transformation for improved accuracy

591   of soil particle-size fraction mapping, Geoderma, 324, 56-66, https://doi.org/10.1016/j.geoderma.2018.03.007, 2018.

592   Yang, R.-M., Zhang, G.-L., Liu, F., Lu, Y.-Y., Yang, F., Yang, F., Yang, M., Zhao, Y.-G., and Li, D.-C.: Comparison of boosted

593   regression tree and random forest models for mapping topsoil organic carbon concentration in an alpine ecosystem,

594   Ecological Indicators, 60, 870-878, https://doi.org/10.1016/j.ecolind.2015.08.036, 2016.

595   Yi, C., Li, D., Zhang, G., Zhao, Y., Yang, J., Liu, F., and Song, X.: Criteria for partition of soil thickness and case studies, Acta

596   Pedologica Sinica, 52, 220-227, 2015.

597   Yue, T., Liu, Y., Zhao, M., Du, Z., and Zhao, N.: A fundamental theorem of Earth's surface modelling, Environ. Earth Sci., 75,

598   751, https://doi.org/10.1007/s12665-016-5310-5, 2016.

599   Yue, T., Zhao, N., Liu, Y., Wang, Y., Zhang, B., Du, Z., Fan, Z., Shi, W., Chen, C., Zhao, M., Song, D., Wang, S., Song, Y.,

600   Yan, C., Li, Q., Sun, X., Zhang, L., Tian, Y., Wang, W., Wang, Y. a., Ma, S., Huang, H., Lu, Y., Wang, Q., Wang, C., Wang,

601   Y., Lu, M., Zhou, W., Liu, Y., Wang, Z., Bao, Z., Zhao, M., Zhao, Y., Rao, Y., Naseer, U., Fan, B., Li, S., Yang, Y., and

602   Wilson, J. P.: A fundamental theorem for eco-environmental surface modelling and its applications, Science China-Earth

603   Sciences, 63, 1092-1112, https://doi.org/10.1007/s11430-019-9594-3, 2020.

604   Yue, T.: Surface Modelling: High accuracy and high speed methods. New York: CRC Press, 2011.

605   Yue, T., Du, Z., Song, D., and Gong Y.: A new method of surface modeling and its application to DEM construction.

606   Geomorphology 91 (1-2): 161-172, 2007.

607   Zhang, M., Shi, W., and Xu, Z.: Systematic comparison of five machine-learning models in classification and interpolation of

608   soil particle size fractions using different transformed data, Hydrol. Earth Syst. Sci., 24, 2505-2526,

609   https://doi.org/10.5194/hess-24-2505-2020, 2020.